eLife

Reviewed Preprint
v1 • March 18, 2025
Not revised

Developmental Biology

Pu.1/Spi1 dosage controls the turnover and maintenance of microglia in zebrafish and mammals

Yi Wu, Weilin Guo, Haoyue Kuang, Xiaohai Wu, Yuexin Wang, Shizheng Zhao, Zilong Wen, Tao Yu

Biomedical Research Institute, Shenzhen Peking University-the Hong Kong University of Science and Technology Medical Center, Shenzhen, China • Division of Life Science, the Hong Kong University of Science and Technology, Hong Kong, China • Greater Bay Biomedical Innocenter, Shenzhen Bay Laboratory, Shenzhen, China

eLife Assessment

This study presents **valuable** findings on the control of survival and maintenance of a specific set of brain resident immune cells. The authors generate a new animal model to enable sophisticated analysis of cell function in vivo. The sophisticated knock-in/knock-out alleles are **compelling**, although the work would ultimately be strengthened with further mechanistic analyses.

https://doi.org/10.7554/eLife.105788.1.sa3

Abstract

Microglia are brain-resident macrophages playing pivotal roles in CNS development and homeostasis. Yet, the cellular and molecular basis governing microglia maintenance remain largely unknown. Here, via utilizing a visible conditional knockout allele of *pu.1* gene (the master regulator for microglia/macrophage lineage development) to generate mosaic microglia populations in adult zebrafish, we show that while *pu.1*-deficient microglia are immediate viable, they are less competitive and chronically eliminated through Tp53-mediated cell competition. Interestingly, when conditionally inactivating Pu.1 in adult *spi-b* (the paralogue of zebrafish Pu.1) null mutants, microglia are rapidly depleted via apoptosis, suggesting that Pu.1 and Spi-b regulate microglia maintenance in a dosage-dependent manner. The dosage-dependent regulation of microglia maintenance by PU.1 is evolutionarily conserved in mice, as shown by conditionally inactivating single and both *Pu.1* alleles in microglia respectively. Collectively, our study reveals the conserved cellular and molecular mechanisms controlling microglia turnover and maintenance in teleost and mammals.

Introduction

Microglia, the crucial immune cells residing in the central nervous system (CNS), have a profound impact on the maintenance of CNS homeostasis, as they not only function as scavengers to facilitate the removal of invading pathogens or damaged tissues, but also actively regulate

neurogenesis, synaptic pruning and neuronal activity (Colonna & Butovsky, 2017; Gomez-Nicola & Perry, 2015). It is therefore not surprising that the dysfunction of microglia is closely linked with the occurrence and progression of many neurodegenerative disorders (Glass *et al*, 2010; Li *et al*, 2012; Prinz *et al*, 2011), thus making it a promising therapeutic target in the prevention and treatment of these diseases.

In mice, fate-mapping methods revealed that unlike other glia cells with neuroectoderm origin, microglia in adult originate from yolk-sac (YS) derived primitive macrophages, which colonize the developing brain rudiment during early embryogenesis (Ginhoux *et al*, 2010; Schulz *et al*, 2012). Whether microglia in adult mammals were contributed by monocyte-derived microglia precursors had long been a debate until the establishment of parabiosis assay (Ajami *et al*, 2007). It is now well-accepted that under physiological condition microglia in mice are maintained locally by self-renewal throughout the lifespan. In accordance with this concept, microglia population was found to be rapidly reconstituted by resident cells after genetic or pharmacological ablation of microglia (Bruttger *et al*, 2015; Elmore *et al*, 2014). However, when estimating the physiological turnover rate of microglia via different methods such as ^{3}H-thymidine/BrdU/EdU incorporation, Ki67 staining or two photon live imaging, different studies yielded distinct or even contradictory results i.e., the estimated microglia turnover rate ranging from 0.13 to 0.8% (Askew *et al*, 2017; Füger *et al*, 2017; Lawson *et al*, 1992; Tay *et al*, 2017), which indicated that microglia in adult mice (~2 years lifespan) were either long-lived without replenishment or replenished for several times during the whole lifespan of the animals. Nonetheless, these studies have reached the consensus that in adult mice all microglia have the proliferation capability and there are no putative microglia precursors existing to proliferate asymmetrically and continuously to contribute to microglia pool. Moreover, microglia proliferation had been shown to be spatially and temporally coupled with apoptosis to maintain the homeostasis of their population (Askew *et al*., 2017): which indicates that not only proliferating microglia locate near the dying microglia, but also newborn microglia manifest a higher frequency of apoptosis. However, whether this phenomenon is for the quality control of microglia or has any other physiological relevance remained unclear. In addition, as a fraction of newborn microglia underwent apoptosis and did not contribute to microglia homeostasis, previously calculated proliferation rate might potentially over-estimate the true turnover rate of microglia. Collectively, although these studies give some insights into the understanding of microglia turnover and maintenance, our knowledge about the underlying cellular and molecular mechanisms are still limited.

PU.1/SPI1, the founding member of the spleen focus forming virus proviral integration oncogene (SPI) subfamily of the E-twenty six (ETS) family transcription factor, is one of the best-characterized gene governing the development of macrophage lineage (McKercher *et al*, 1996; Scott *et al*, 1994). Disruption of PU.1 in mice causes early lethality of the embryos and complete absence of macrophages (McKercher *et al*., 1996; Scott *et al*., 1994), including microglia in brain (Kierdorf *et al*, 2013). Interestingly, the *PU.1* expression level was found to remain at a high level in microglia after their terminal differentiation (Walton *et al*, 2000), implying that PU.1 also regulates the cellular behaviors and functions of microglia in the sophisticated CNS environment. Indeed, Chromatin immunoprecipitation (ChIP)-Seq analysis with microglia cell line BV2 cells revealed thousands of PU.1 targets (Satoh *et al*, 2014). Accordingly, silencing of PU.1 by siRNA in mixed human glial culture led to the reduced viability of microglia and decreased phagocytosis of amyloid-beta (Aβ42) (Smith *et al*, 2013). However, as a previous study reported that inactivating either 1 copy or 2 copies of PU.1 by fusing PU.1 with cytoplasm-retaining estrogen receptor (ER) had no effect on the viability of alveolar macrophages (Karpurapu *et al*, 2011), whether PU.1 indeed regulated the survival and maintenance of microglia in the in-vivo conditions remained to be further investigated. Moreover, human SNPs that altered *PU.1* expression level were reported to be associated with Alzheimer's disease (AD) pathogenesis (Cao *et al*, 2022; Huang *et al*, 2017). A recent study showed that conditional inactivation or pharmacological inhibition of PU.1 in AD mouse model ameliorated neuroinflammation, prevented microgliosis and improved cognitive performance (Ralvenius *et al*, 2023). Although reduction of microglia number was

considered as a result of the amelioration of neuroinflammation, whether PU.1 directly regulated microglia survival and maintenance to prevent the propagation of neuroinflammation in diseased condition deserved to be carefully revisited. SPI-B, another member in the mammalian SPI subfamily, has been shown to be dispensable for the development of the macrophage lineage (Su *et al*, 1997). Yet, its involvement in the regulation of microglia turnover and maintenance remains to be investigated.

Owing to the genetic amenability and the feasibility for live-imaging and lineage tracing, zebrafish has been adopted as an ideal model for the study of microglia development and function (Hughes & Appel, 2020; Iyer *et al*, 2022; Li *et al*., 2012; Peri & Nüsslein-Volhard, 2008). Zebrafish microglia are highly conserved with their mammalian counterparts in terms of morphology, molecular signatures, development-regulatory genetic networks as well as functions (Xu *et al*, 2015; Yu *et al*, 2017). Different from the single origin of mouse microglia, zebrafish microglia were shown to arise from two distinct sources i.e., the rostral blood (RBI), equivalent of mouse YS for primitive myelopoiesis, and the aorta-gonad-mesonephros (AGM) region for hematopoietic stem cell (HSC) initiation. The RBI microglia colonize the developing brain during early embryogenesis, but are gradually replenished by AGM adult microglia (Xu *et al*., 2015). Further study revealed that this dynamic shift of microglia pool is controlled by Il34-Csf1ra signaling-dictated cell competition (Yu *et al*, 2023). Yet, when the microglia pool is established in adult zebrafish, the molecular mechanisms underlying their turnover and maintenance remain incompletely understood. Moreover, although Pu.1 (also called Spi1b) and its paralogue Spi-b (also called Spi1a), the zebrafish orthologues of mammalian PU.1 and SPI-B, were shown to be indispensable for microglia early development of both origins in zebrafish (Xu *et al*., 2015; Yu *et al*., 2017), their functions in the survival and maintenance of microglia in adult animals have not been established.

In the present study, via the condition knockout strategy to generate mosaic microglia population in adult zebrafish and mice, we revealed that the turnover and maintenance of microglia is evolutionarily conserved and regulated by Pu.1/Spi1 dosage from teleost to mammals.

Results

Adult microglia in zebrafish undergo rapid turnover and random proliferation to replenish and maintain their pool

Previous studies have shown that there are two major subtypes of myeloid cells, i.e., *ccl34b.1*$^+$ microglia and *ccl34b.1*$^-$*ccl19a.1*$^+$ brain-resident dendritic cells (DCs) in adult zebrafish brain (Wu *et al*, 2020; Zhou *et al*, 2023). To monitor the turnover and maintenance of microglia in adult zebrafish brain, we employed microglia-specific *TgBAC(ccl34b.1:eGFP)* transgenic reporter line (Wu *et al*., 2020) and performed EdU pulse-chase experiment, a similar strategy with that in mouse to determine microglia turnover (Askew *et al*., 2017; Tay *et al*., 2017). As a single dose of EdU injection might under-estimate the microglia turnover rate, we intraperitoneally injected EdU into adult *TgBAC(ccl34b.1:eGFP)* fish for either 1, 3 or 5 consecutive days. We then collected the fish brain at 1 day post injection (dpi) for cryosection and co-staining of eGFP, Lcp1 (a pan leukocyte marker expressed in both microglia and DCs), EdU and DAPI, in which ccl34b.1-eGFP$^+$Lcp1$^+$ cells are microglia and ccl34b.1-eGFP$^-$Lcp1$^+$ cells represent DCs (**Fig. 1A**). Quantification results showed that, while a single dose of EdU pulse labeled 1.892±0.234% microglia, the EdU incorporate rate for microglia after 3 or 5 doses of EdU pulses increased almost linearly (**Fig. 1B**, green bars). Based on these data, the estimated microglia turnover rate (daily) is ~2.6% (total EdU incorporation rate divided by the times of EdU-pulses) (**Fig. 1C**, green bars). On the other hand, the EdU incorporate rate for the DCs was much lower (**Fig. 1B-C**, red bars), suggesting that the DCs in the brain are relatively steady with a very low turnover rate.

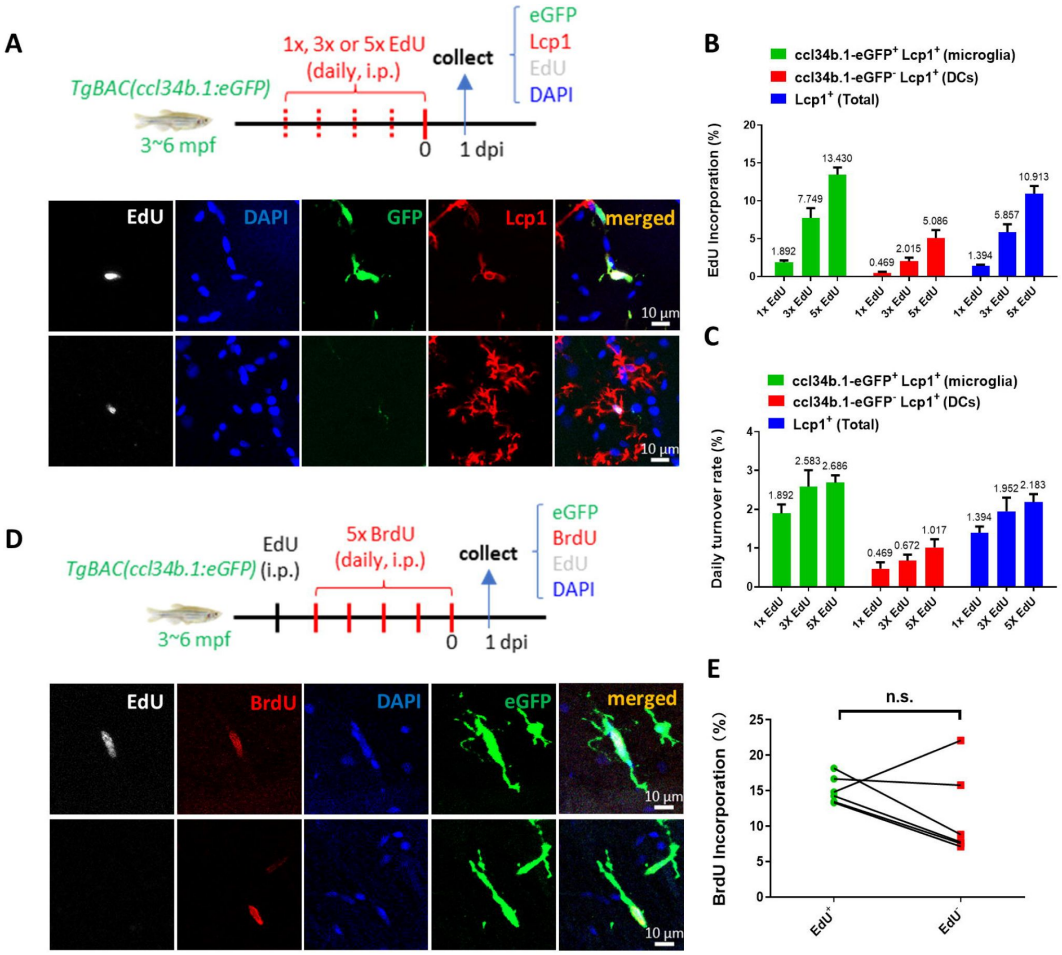

Fig. 1.

Adult microglia in zebrafish undergo rapid turnover and random proliferation to replenish and maintain their pool.

(A) Schematic diagram shows the workflow of EdU pulse experiment in adult *TgBAC(ccl34b.1:eGFP)* zebrafish and the representative images of proliferating microglia (ccl34b.1-eGFP$^+$ Lcp1$^+$EdU$^+$) and dendritic cells (DCs) (ccl34b.1-eGFP$^-$ Lcp1$^+$EdU$^+$) in the midbrain. **(B)** Quantification of the EdU incorporation proportions in microglia and DCs with different dosages of EdU pulses. (n=4 for each group) **(C)** The daily turnover rate of microglia and DCs calculated by dividing the EdU incorporation rate with EdU pulses. **(D)** Schematic diagram shows the experimental setup for EdU-BrdU double-pulse in adult wild-type fish and the representative images shows two BrdU$^+$ microglia with or without EdU incorporation. **(E)** Comparison of BrdU incorporation proportions in EdU$^+$eGFP$^+$ and EdU$^-$eGFP$^+$ microglia (n=6). n.s. = not significant, p>0.05.

Previously, via the EdU/BrdU dual-pulse assay, Tay et al. have shown that microglia in adult mouse brain proliferate randomly during homeostasis and no putative microglia precursors have been identified accordingly (Tay *et al*., 2017). To clarify whether there might be putative microglial precursors that continuously proliferate to contribute to microglia turnover in zebrafish, we employed a similar strategy, in which adult wild-type (WT) fish were injected with a single dose of EdU followed with five daily BrdU pulses to determine the BrdU proliferation rate of EdU^+ and EdU^- microglia (**Fig. 1D**, upper panel). Quantification result showed that the BrdU incorporation rates were comparable between EdU^+ and EdU^- microglia pools (**Fig. 1D-E**). These data strongly suggest that, similar to mammals (Tay *et al*., 2017), microglia in adult zebrafish randomly undergo proliferation and there are no well-defined microglial precursors that continuously proliferate to replenish and maintain the microglia pool.

Generation and characterization of the visible conditional knockout allele *pu.1^{KI}*

To elucidate the molecular mechanisms underlying microglia turnover and maintenance, we focused on the Ets family transcription factor PU.1/SPI1, which had been shown to be a master regulator for macrophage/microglia development in fish and mammals (McKercher *et al*., 1996; Scott *et al*., 1994; Yu *et al*., 2017). Because macrophages/microglia development is completely blocked at early development in *pu.1*-null zebrafish mutants (Yu *et al*., 2017), we decided to generate a visible *pu.1* conditional knockout allele *pu.1^{KI}*to study the role of Pu.1 in microglia maintenance via the Non-homologous end jointing (NHEJ)-mediated knock-in method (**Fig. 2A** and Fig. S1A) (Li *et al*, 2015). As shown in **Fig. 2A**, the knock-in DNA fragment consisted of loxP, *pu.1* exon 4 to 6 followed by the self-cleaving P2A sequence-conjugated eGFP, and a splicing-acceptor site SpA2 followed by the P2A-DsRed. In addition, the 3' downstream sequence of *pu.1* gene (gray box) was added to the 3' end of each fluorescent protein to ensure efficient termination of RNA transcription and proper expression of the fluorescent proteins.

Three different founders were obtained. PCR and deep sequencing analysis of F1 embryos confirmed the correct integration of donor DNA fragment in the *pu.1* locus (Fig. S1B-C). Since the knock-in *pu.1^{KI}* allele would generate intact Pu.1 and eGFP concurrently (**Fig. 2A**), we predicted the expression pattern of eGFP, which presumably represents the expression of the knock-in Pu.1, should completely overlap with the endogenous Pu.1. Indeed, co-staining of eGFP and Pu.1 antibodies revealed a perfect overlap of the $eGFP^+$ cells and $Pu.1^+$ cells in *pu.1$^{KI/+}$* embryos (**Fig. 2B**), suggesting that the *pu.1^{KI}* allele recapitulates the expression of endogenous *pu.1*. Further studies suggested that *pu.1^{KI}-eGFP* efficiently labels embryonic microglia, and both microglia and DCs in adult, as revealed by the co-localization of *pu.1^{KI}-eGFP* and macrophage-specific reporter line *Tg(mpeg1:LRLG)* at 3 dpf, and by the co-staining of eGFP and Lcp1 antibodies on the brain sections of adult *pu.1$^{KI/+}$* fish respectively (**Fig. 2C and D**). To further confirm functional intactness of the *pu.1^{KI}* allele, we crossed the *pu.1^{KI}* fish with the *pu.1$^{\Delta 839}$* mutants to examine if the *pu.1^{KI}*allele is capable of rescuing the microglia phenotype. Indeed, quantification of microglia number revealed no difference between the *pu.1$^{\Delta 839/KI}$* and *pu.1$^{\Delta 839/+}$* embryos (**Fig. 2E and F**), indicating that the *pu.1^{KI}* allele functionally recapitulates the endogenous *pu.1*.

To test whether the Cre mediated excision occurs correctly in the *pu.1^{KI}* allele, we injected Cre mRNA into the *pu.1^{KI}* embryos at one-cell stage. The injected embryos were raised to adulthood (*pu.1^{CKO}* fish) and crossed with the *pu.1^{KI}* fish to generate *pu.1$^{CKO/KI}$* fish. As illustrated in **Fig. 2A**, the Cre-mediated excision should remove the E4-6-P2A-eGFP cassette and allow the proper splicing of the splicing-acceptor site SpA2 and joining of the P2A-DsRed with exon 3 (**Fig. 2A**), leading to the induction of DsRed expression. Indeed, fluorescent imaging of the *pu.1$^{CKO/KI}$* embryos revealed robust DsRed (*pu.1^{CKO}* allele) signals perfectly overlapping with the eGFP (*pu.1^{KI}* allele) signals (**Fig 2G**), suggesting the correct DNA excision and RNA splicing in the *pu.1^{CKO}* allele. This conclusion was further validated by sequencing analysis of the *pu.1^{CKO}* transcripts (**Fig. 2H**). Since the endogenous *pu.1* exons were not replaced, but instead they were

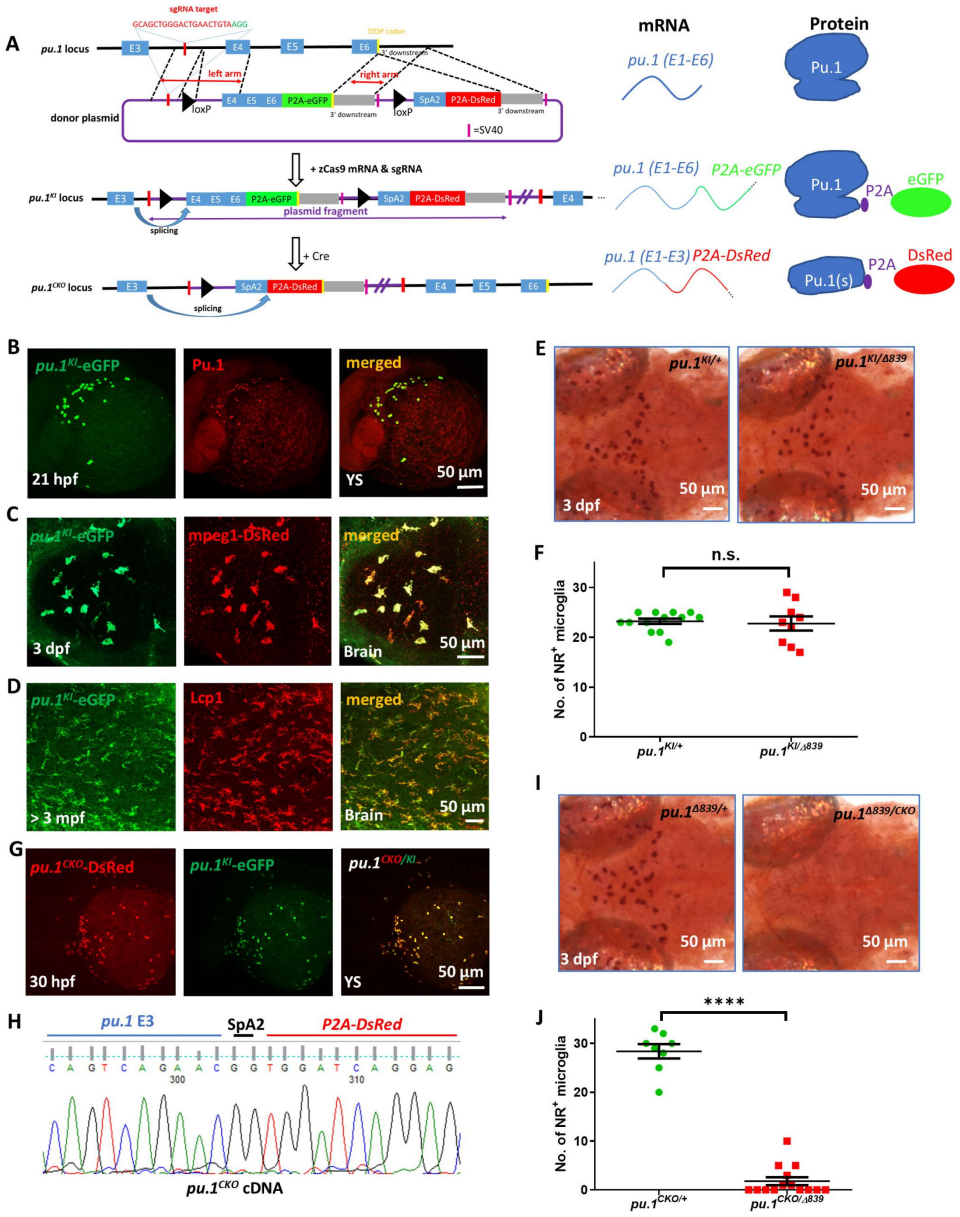

Fig. 2.

Generation and characterization of the visible conditional knockout allele *pu.1*^{KI}.

(A) Schematic diagrams show the generation of *pu.1*^{KI} allele and the principle for *pu.1* visible conditional knockout. Briefly, the donor plasmid, which contains: (1) the sgRNA target sequence in *pu.1* intron 3~4; (2) the loxP-flanked *pu.1* coding sequence (exon4-6) followed by P2A-eGFP; (3) the splicing acceptor site followed by P2A-DsRed sequence was knocked into the endogenous *pu.1* locus via non-homologous end joining (NHEJ) to generate *pu.1*^{KI}. In principle, the splicing event occurring between E3 and E4 In *pu.1*^{KI} would produce intact Pu.1 and eGFP concurrently. After Cre-mediated recombination, removal of *pu.1* E4-6 and splicing of P2A-DsRed sequence in *pu.1*^{CKO}allele leads to the disruption of Pu.1 and fluorescent color change. **(B)** Co-staining of anti-eGFP and anti-Pu.1 antibodies on the yolk sac (YS) of 21-hpf *pu.1*^{KI} embryos. **(C)** Fluorescent imaging of the optic tectum (OT) region of 3-dpf *pu.1*^{KI}*;Tg(mpeg1:LRLG)* embryos. **(D)** Co-staining of anti-eGFP and anti-Lcp1 antibodies on the midbrain cross section of adult *pu.1*^{KI} fish. **(E)** Neutral red staining of *pu.1*$^{KI/+}$ and *pu.1*$^{KI/Δ839}$ embryos at 3 dpf. **(F)** Quantification of NR^{+} microglia in *pu.1*$^{KI/+}$ (n=13) and *pu.1* $^{KI/Δ839}$ (n=9) embryos at 3 dpf. **(G)** Fluorescent imaging of the YS region of 30-hpf *pu.1*$^{KI/CKO}$ embryos. **(H)** Chromogram of cDNA sequence from *pu.1*^{CKO} embryos shows the precise splicing of *P2A-DsRed* cassette to *pu.1* E3. **(I)** Neutral red staining of *pu.1*$^{CKO/+}$ and *pu.1*$^{CKO/Δ839}$ embryos at 3 dpf. **(J)** Quantification of NR^{+} microglia in *pu.1*$^{CKO/+}$ (n=8) and *pu.1*$^{CKO/Δ839}$ embryos at 3 dpf (n=14). n.s. = not significant, p>0.05; ****p<0.0001.

separated far away from the upstream exons by donor plasmid, we performed quantitative RT-PCR analysis of *pu.1*$^{CKO/CKO}$ embryos to determine the possible expression of the endogenous *pu.1* exons in *pu.1*^{CKO}allele. The result showed that the relative expression of endogenous *pu.1* exons is around 1~2% in comparison with that of DsRed expression (Fig. S1D), suggesting that expression of *pu.1* is largely abolished in *pu.1*^{CKO} allele. To phenotypically characterize *pu.1*^{CKO} allele, and to avoid incomplete inactivation of Pu.1 function in downstream microglia tracing experiments, which may occur when using two *pu.1*^{KI} alleles due to the lower CreER recombination efficiency in zebrafish compared to mice, we outcrossed the *pu.1*^{CKO} fish with the *pu.1*$^{\Delta 839}$ null mutants. As anticipated, the development of embryonic microglia was completely blocked in the *pu.1*$^{CKO/\Delta 839}$ embryos (**Fig. 2I and J**), a phenotype recapitulating the defect of the *pu.1*$^{\Delta 839}$ homozygous mutants (Yu *et al.*, 2017). These data demonstrate that the *pu.1*^{KI} allele works very well and serves as a useful tool to explore the role of Pu.1 in adult microglia survival and maintenance.

Pu.1 and Spi-b regulate the turnover and maintenance of microglia in a dosage-dependent manner

To investigate the role of Pu.1 in the survival and maintenance of microglia in adult zebrafish, we crossed the *pu.1*^{KI} fish with the leukocyte-specific *Tg(coro1a:CreER)* line and the *pu.1*$^{\Delta 839}$ mutants to generate *pu.1*$^{KI/+}$*;Tg(coro1a:CreER)* and *pu.1*$^{KI/\Delta 839}$*;Tg(coro1a:CreER)* fish. We then intraperitoneally injected 3 doses of 4-OHT into these adult fish and collected the brain samples at 2 dpi and 8 dpi for the quantification of microglia number after cryo-section and eGFP/DsRed immuno-staining (**Fig. 3A**, upper panel). As shown in **Fig. 3A** (lower panel), DsRed^{+} cells were readily detected in the brains of both *pu.1*$^{KI/+}$*;Tg(coro1a:CreER)* and *pu.1*$^{KI/\Delta 839}$*;Tg(coro1a:CreER)* fish at 8 dpi. Quantification of the number and proportion of DsRed^{+} cells at 2 dpi and 8 dpi revealed no difference between *pu.1*$^{KI/\Delta 839}$*;Tg(coro1a:CreER)* mutant fish and *pu.1*$^{KI/+}$*;Tg(coro1a:CreER)* control siblings (**Fig. 3B-C**). In accordance with this observation, we also found that the number and proportion of microglia (ccl34b.1-eGFP^{+} Lcp1^{+}) and DCs (ccl34b.1-eGFP^{-}Lcp1^{+}) were comparable between *pu.1*$^{\Delta 839/\Delta 839}$*;TgBAC(ccl34b.1:eGFP)* null mutants and *pu.1*$^{\Delta 839/+}$*;TgBAC(ccl34b.1:eGFP)* siblings (Fig. S2). These data suggest that Pu.1 is not required for the survival of microglia and DCs. We reasoned that the survival of *pu.1*-deficient microglia is likely attributed to the presence of *spi-b* (the paralogue of *pu.1* in zebrafish, also called *spi1a*), which has been shown to play a compensatory role for Pu.1 in microglia early development (Yu *et al.*, 2017). Indeed, conditional inactivation of Pu.1 in the *spi-b*$^{\Delta 232/\Delta 232}$ null mutants led to a rapid depletion of microglia by apoptosis within several days (Fig. S3 and Fig. S4), indicating that Pu.1 and Spi-b act redundantly to regulate the survival of microglia.

To further investigate whether Pu.1-deficiency might have a long-term effect on the turnover and maintenance of microglia, we traced *pu.1*-deficient DsRed^{+} cells to 1 month post injection (mpi), and 3 mpi after conditionally inactivating Pu.1 in adult *pu.1*$^{KI/+}$*;Tg(coro1a:CreER)* and *pu.1*$^{KI/\Delta 839}$*;Tg(coro1a:CreER)* fish (**Fig. 3D**, upper panel). Intriguingly, we found that the number and proportion of DsRed^{+} cells in the midbrains of the *pu.1*$^{KI/\Delta 839}$*;Tg(coro1a:CreER)* fish began to decline at 1 mpi and were further reduced, becoming significantly lower than that in *pu.1*$^{KI/+}$*;Tg(coro1a:CreER)* fish by 3 mpi (**Fig.3E**-F). Likewise, the number and proportion of DsRed^{+} cells in the retina and spinal cord were also significantly reduced in the *pu.1*$^{KI/\Delta 839}$*;Tg(coro1a:CreER)* fish by 3 mpi (Fig. S5). Since microglia are the major population of the *coro1a*$^{+}$ cells in the brain and spinal cord and the exclusive population in the retina (Wu *et al.*, 2020), the reduction of DsRed^{+} cells in the *pu.1*$^{KI/\Delta 839}$*;Tg(coro1a:CreER)* fish at 1 mpi and 3 mpi are mainly attributed to the loss of microglia. Based on the amoeboid and ramified morphology, microglia and DCs could be distinguished with about 90% accuracy (Fig. S6A-B). Thus, to further confirm above conclusion, we quantified microglia and DCs separately in 3-mpi *pu.1*$^{KI/+}$*;Tg(coro1a:CreER)* and *pu.1*$^{KI/\Delta 839}$*;Tg(coro1a:CreER)* fish. As anticipated, *pu.1*-deficient microglia were significantly reduced at 3 mpi (Fig. S6C-D). These results suggest that, although *pu.1*

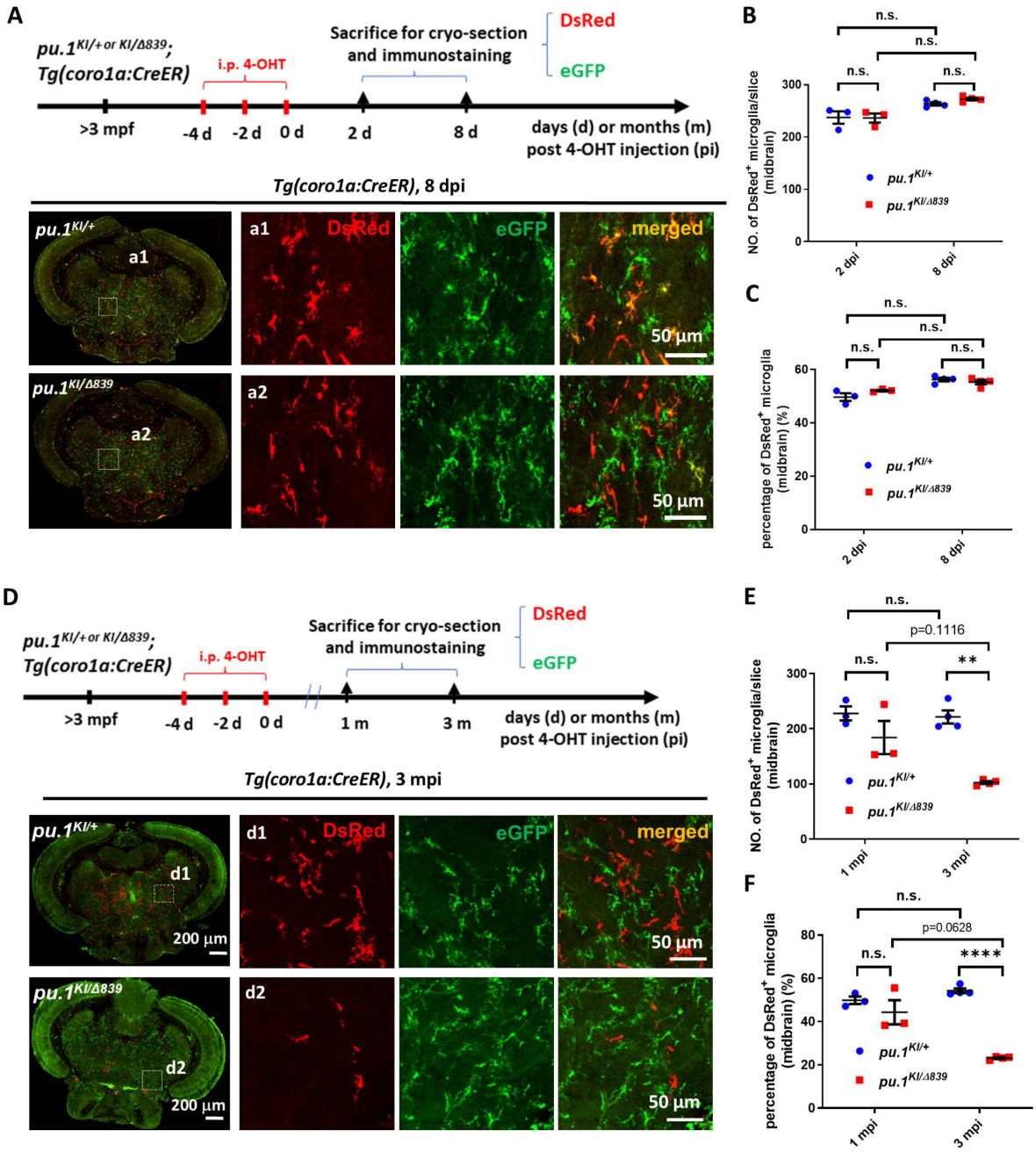

Fig. 3.

pu.1-deficient microglia were chronically eliminated in mosaic condition.

(A) The experimental setup for *pu.1* conditional knockout in adult zebrafish and the representative images of midbrain cross section of *pu.1*$^{KI/+}$*;Tg(coro1a:CreER)* and *pu.1*$^{KI/\Delta839}$*;Tg(coro1a:CreER)* fish at 8 days post 4-OHT injection (dpi). **(B)** Quantification of the number of DsRed^{+} microglia on the midbrain cross section of *pu.1*$^{KI/+}$*;Tg(coro1a:CreER)* and *pu.1*$^{KI/\Delta839}$*;Tg(coro1a:CreER)* fish at 2 dpi (n=3) and 8 dpi (n=4). **(C)** Quantification of the proportion of DsRed^{+} microglia on the midbrain cross section of *pu.1*$^{KI/+}$*;Tg(coro1a:CreER)* and *pu.1*$^{KI/\Delta839}$*;Tg(coro1a:CreER)* fish at 2 dpi (n=3) and 8 dpi (n=4). **(D)** The experimental setup for *pu.1* conditional knockout in adult zebrafish and the representative images of midbrain cross section of *pu.1*$^{KI/+}$*;Tg(coro1a:CreER)* and *pu.1*$^{KI/\Delta839}$*;Tg(coro1a:CreER)* fish at 3 months post 4-OHT injection (mpi). **(E)** Quantification of the number of DsRed^{+} microglia on the midbrain cross section of *pu.1*$^{KI/+}$*;Tg(coro1a:CreER)* and *pu.1*$^{KI/\Delta839}$*;Tg(coro1a:CreER)* fish at 1 mpi (n=3) and 3 mpi (n=4). **(F)** Quantification of the proportion of DsRed^{+} microglia on the midbrain cross section of *pu.1*$^{KI/+}$*;Tg(coro1a:CreER)* and *pu.1*$^{KI/\Delta839}$*;Tg(coro1a:CreER)* fish at 1 mpi (n=3) and 3 mpi (n=4). n.s. = not significant, p>0.05; **p<0.01; ****p<0.0001.

is dispensable for the immediate survival of microglia (**Fig. 3B-C**), it is essential for the turnover and long-term maintenance of microglia in adult zebrafish, which could not be fully compensated by *spi-b*.

pu.1-deficient microglia in mosaic condition were eliminated by cell competition

Given the fact that *pu.1*-deficient microglia are gradually eliminated in mosaic condition (**Fig. 3E-F**), but their number remains relatively normal in $pu.1^{\Delta 839}$ null mutants (Yu *et al*., 2017), we reasoned that the elimination of the *pu.1*-deficient microglia in mosaic condition is likely attributed to the cell competition between *pu.1*-deficient DsRed$^+$ microglia and their neighboring eGFP$^+$ sibling cells harboring WT *pu.1*. To test this hypothesis, we compared the cell death and proliferation rates of microglia by TUNEL and BrdU incorporation assays in both conditions respectively. To determine the cell death and proliferation rates of *pu.1*-deficient microglia in mosaic condition, we treated the adult $pu.1^{KI/\Delta 839}$*;Tg(coro1a:CreER)* fish with 4-OHT to inactivate Pu.1. At 26 dpi, the 4-OHT-treated fish were then injected 5 doses (one dose daily) of BrdU and the brain samples were collected 1 day later for TUNEL and BrdU staining respectively (**Fig. 4A**). Quantification results showed that the percentage of TUNEL$^+$DsRed$^+$ microglia (*pu.1*-deficient cells) in the brains of the $pu.1^{KI/\Delta 839}$*;Tg(coro1a:CreER)* fish was significantly higher than that of TUNEL$^+$eGFP$^+$ cells (**Fig. 4B**). In this assay, the 4-OHT-treated $pu.1^{KI/+}$*;Tg(coro1a:CreER)* fish were included as the control, and as expected, the percentages of TUNEL$^+$ cells in the DsRed$^+$ and eGFP$^+$ microglia pools in control fish were comparable (**Fig. 4B**). In parallel, we also found that the BrdU incorporation rates of *pu.1*-deficient microglia (DsRed$^+$) in the 4-OHT-treated $pu.1^{KI/\Delta 839}$*;Tg(coro1a:CreER)* fish was significantly lower than that of eGFP$^+$ cells (**Fig. 4C**), while the BrdU incorporation rates of DsRed$^+$ cells and eGFP$^+$ cells in the control $pu.1^{KI/+}$*;Tg(coro1a:CreER)* fish was comparable (**Fig. 4C**). These results indicate that conditional inactivation of Pu.1 in adult zebrafish leads to the impairment of cell proliferation and accelerated cell death of microglia in mosaic condition. To estimate the cell death and proliferation rates of microglia in *pu.1*-null mutants, we utilized a similar strategy via pulsing the adult $pu.1^{\Delta 839/+}$*;TgBAC(ccl34b.1:eGFP) or* $pu.1^{\Delta 839/\Delta 839}$*;TgBAC(ccl34b.1:eGFP)* fish with 5 doses of BrdU (daily) and collecting the brains samples at 1 day later for TUNEL and BrdU staining respectively (**Fig. 4D**). As shown in **Fig. 4E**, the percentage of TUNEL$^+$ccl34b.1-eGFP$^+$ microglia showed no difference between $pu.1^{\Delta 839/\Delta 839}$ mutants and $pu.1^{\Delta 839/+}$ siblings, demonstrating that the intrinsic viability of *pu.1*-deficient microglia in the null mutants was largely unaffected. Similarly, the proliferation capability (as indicated by BrdU incorporation rate) of *pu.1*-deficient microglia in the null mutants remained normal as well in comparison with control siblings (**Fig. 4F**). Collectively, these results strongly suggest that the chronic elimination of *pu.1*-deficient DsRed$^+$ microglia is indeed caused by cell competition, which only occurs in the mosaic condition when the eGFP$^+$ microglia harboring a single copy of *pu.1* are present.

The out-competition of *pu.1*-deficient microglia in mosaic condition is mediated by Tp53

To uncover the key downstream targets that mediate the out-competition of *pu.1*-deficient DsRed$^+$ microglia in mosaic condition, we manually picked DsRed$^+$ and eGFP$^+$ microglia from the 4-OHT-treated $pu.1^{KI/\Delta 839}$*;Tg(coro1a:CreER)* fish at 3 mpi and performed transcriptomic analysis (**Fig. 5A**). To minimize the contamination of DCs, we manually picked 3∼5 DsRed$^+$ or GFP$^+$ cells from the brain suspension of 3-mpi $pu.1^{KI/\Delta 839}$*;Tg(coro1a:CreER)* fish in each tube for cDNA library construction and RNAseq. Samples with strong expression of microglia-related genes and faint DC-related genes were chosen for further analysis (Fig. S7A). Among the differential expressed genes (DEGs), the tumor suppressor gene *tp53* was one of the top targeted genes robustly upregulated in *pu.1*-deficient DsRed$^+$ microglia (**Fig. 5B-C**, Fig. S7B). Interestingly, recent studies have revealed that, in addition to regulating cell cycle arrest and apoptosis in DNA damage response (Ou &

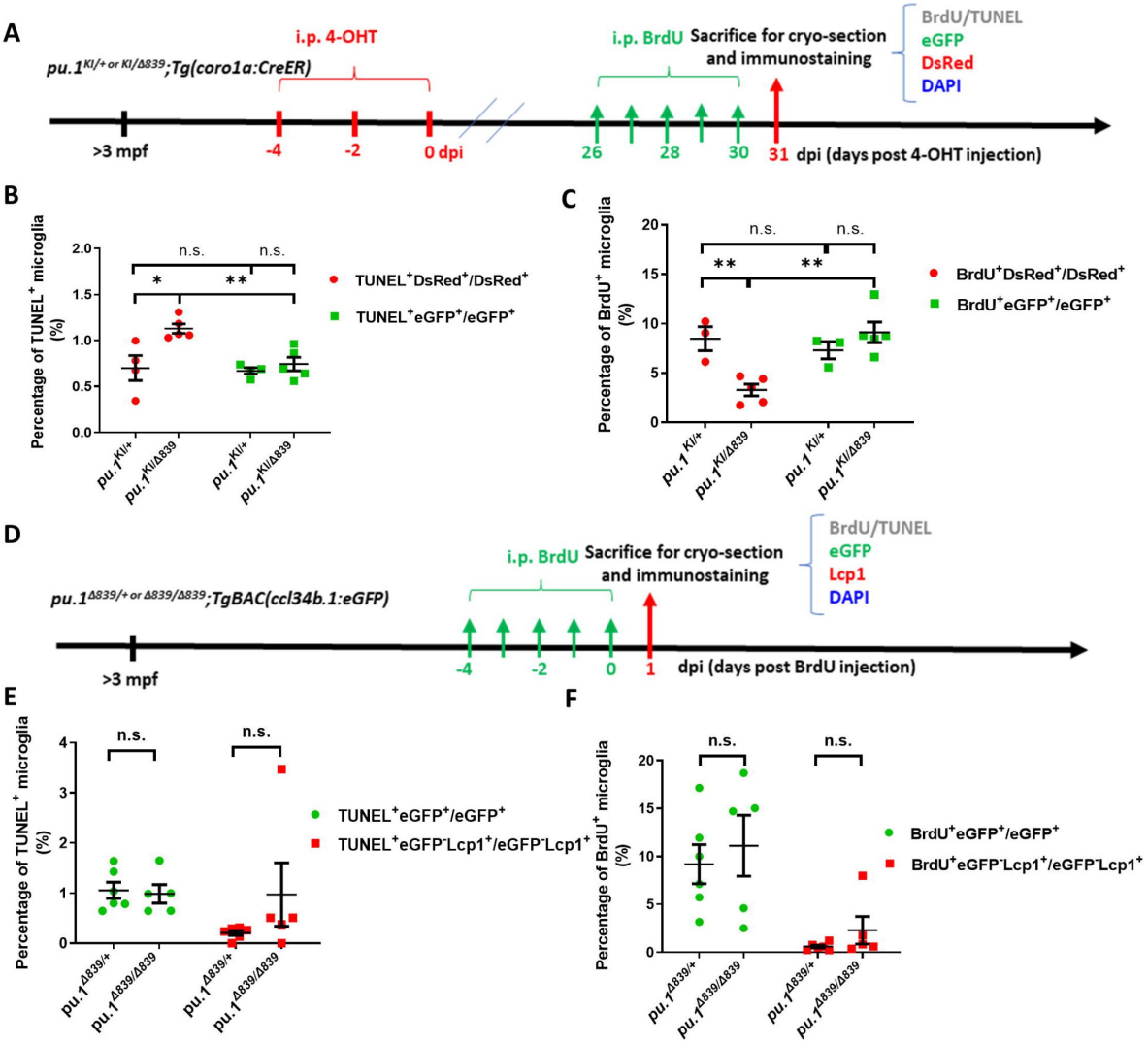

Fig. 4.

pu.1-deficient microglia in mosaic condition were eliminated by cell competition.

(A) The experimental setup for BrdU incorporation and TUNEL assays in adult *pu.1*$^{KI/+}$*;Tg(coro1a:CreER)* and *pu.1*$^{KI/\Delta839}$*;Tg(coro1a:CreER)* fish at 1 mpi. **(B)** Quantification of the percentage of TUNEL$^+$ cells in eGFP$^+$ and DsRed$^+$ microglia in *pu.1*$^{KI/+}$*;Tg(coro1a:CreER)* (n=4) and *pu.1*$^{KI/\Delta839}$*;Tg(coro1a:CreER)* (n=5) fish at 1 mpi. **(C)** Quantification of the percentage of BrdU$^+$ cells in eGFP$^+$ and DsRed$^+$ microglia in adult *pu.1*$^{KI/+}$*;Tg(coro1a:CreER)* (n=4) and *pu.1*$^{KI/\Delta839}$*;Tg(coro1a:CreER)* fish at 1 mpi. **(D)** The experimental setup for BrdU incorporation and TUNEL assays in adult *pu.1*$^{\Delta839/+}$*;TgBAC(ccl34b.1:eGFP)* and *pu.1*$^{\Delta839/\Delta839}$*;TgBAC(ccl34b.1:eGFP)* fish. **(E)** Quantification of the percentage of TUNEL$^+$eGFP$^+$ microglia in adult *pu.1*$^{\Delta839/+}$*;TgBAC(ccl34b.1:eGFP)* and *pu.1*$^{\Delta839/\Delta839}$*;TgBAC(ccl34b.1:eGFP)* fish. **(F)** Quantification of the percentage of BrdU$^+$eGFP$^+$ microglia in adult *pu.1*$^{\Delta839/+}$*;TgBAC(ccl34b.1:eGFP)* (n=6) and *pu.1*$^{\Delta839/\Delta839}$*;TgBAC(ccl34b.1:eGFP)* (n=5) fish. n.s. = not significant, p>0.05; *p<0.05; **p<0.01.

Schumacher, 2018; Vaddavalli & Schumacher, 2022), Tp53 is also involved in cell competition regulation in both hematopoietic and non-hemopoietic tissues (Bondar & Medzhitov, 2010; Zhang *et al*, 2017). Hence, we speculated that the cell competition-mediated chronic elimination of *pu.1*-deficient microglia was likely dependent on Tp53. To support this hypothesis, we conditional inactivated Pu.1 to generate mosaic microglia populations in the *tp53*-deficient mutant background and asked if loss of Tp53 could rescue the microglia phenotype (**Fig. 5D**, upper panel). Indeed, results showed that the number of *pu.1*-deficient DsRed^{+} microglia in the 4-OHT-treated *pu.1*$^{KI/\Delta 839}$*;tp53*$^{-/-}$*;Tg(coro1a:CreER)* fish was significantly restored compared with *pu.1*$^{KI/\Delta 839}$*;Tg(coro1a:CreER)* control fish (**Fig. 5D-F**). Collectively, these results demonstrate that the chronic elimination of *pu.1*-deficient microglia in mosaic condition is mediated, at least in part, by the elevation of Tp53 activity, which leads to the reduced proliferation and excessive death of these microglia.

Dosage-dependent regulation of microglia maintenance by PU.1 is evolutionarily conserved from zebrafish to mice

The above data have demonstrated that the long-term maintenance of microglia in adult zebrafish is regulated by Pu.1 in a dosage-dependent manner. We next wondered whether this mechanism is evolutionarily conserved from teleost to mammals. To address this issue, we first examined the expression of *Pu.1* and *Spi-b* in adult murine microglia. Quantitative RT-PCR revealed that in contrast to the robust expression of *Pu.1*, *Spi-b* was barely detectable in microglia (Fig. S8A). We therefore only focused on *Pu.1* and generated a *Pu.1*^{Fl} allele, in which the exon 2 of *Pu.1* gene is flanked by loxP (Fig. S8B-C). The *Pu.1*^{Fl} mice were then crossed with the *Cx3cr1*$^{CreER\text{-}YFP}$ strain (referred to as to *Cx3cr1*^{CreER}hereafter) (Yona *et al*, 2013) to generate *Pu.1*$^{Fl/+}$*;Cx3cr1*^{CreER}and *Pu.1*$^{Fl/Fl}$*;Cx3cr1*^{CreER} mice for conditional PU.1 inactivation study (**Fig. 6A**).

To investigate whether microglia maintenance in adult mice requires PU.1, we intraperitoneally injected tamoxifen (TAM) (Askew *et al*., 2017) into the *Pu.1*$^{Fl/+}$*;Cx3cr1*^{CreER} *and* *Pu.1*$^{Fl/Fl}$*;Cx3cr1*^{CreER}mice, and collected the brain samples at 7 dpi for cryo-section and IBA1 staining (**Fig. 6A**, upper panel). As expected, without TAM, the number of the IBA1^{+} microglia showed no difference in the brain of *Pu.1*$^{Fl/+}$*;Cx3cr1*^{CreER} *and Pu.1*$^{Fl/Fl}$*;Cx3cr1*^{CreER} mice (Fig. S8D-E). However, after TAM injection, the number of the IBA1^{+} microglia in *Pu.1*$^{Fl/Fl}$*;Cx3cr1*^{CreER} mice were drastically reduced compared to that in *Pu.1*$^{Fl/+}$*;Cx3cr1*^{CreER} mice (**Fig. 6A-C**), suggesting that PU.1 is indeed required for the survival of adult microglia, which is similar to the double depletion of *pu.1* and *spi-b* in zebrafish (Fig. S4). To further explore whether partial loss of PU.1 activity could reduce the competitiveness of microglia and impairs the long-term maintenance of microglia in mice, we intraperitoneally injected sub-dosage of TAM into adult *Pu.1*$^{Fl/+}$*;Cx3cr1*^{CreER}mice to generate mosaic microglia populations for long-term tracing. To quantify the proportion of *Pu.1*$^{KO/+}$microglia and *Pu.1*$^{Fl/+}$ microglia, we sorted YFP^{+} microglia from TAM-injected *Pu.1*$^{Fl/+}$*;Cx3cr1*^{CreER} mice at 3 dpi and 3.5 mpi, the timeline similar to previous research in zebrafish. Then we amplified *Pu.1*^{KO} and *Pu.1*^{Fl} alleles in the gDNA pool by PCR for T-clone quantification (**Fig. 6D**). As shown in **Fig. 6E-F**, while the percentage of *Pu.1*$^{KO/+}$ microglia was comparable to *Pu.1*$^{Fl/+}$ microglia at 3 dpi, it was dramatically reduced by 3.5 mpi, suggesting that removal of a single copy of *Pu.1* leads to the chronic elimination of *Pu.1*$^{KO/+}$ microglia, which appears to occur only in the presence of the WT *Pu.1*$^{Fl/+}$ microglia, as PU.1 heterozygous mice show no difference in the viability of tissue resident macrophages (Karpurapu *et al*., 2011). Collectively, these results indicate that the dosage-dependent cell competition-mediated regulation of microglia maintenance by SPI1/PU.1 is evolutionarily conserved from teleost to mammals.

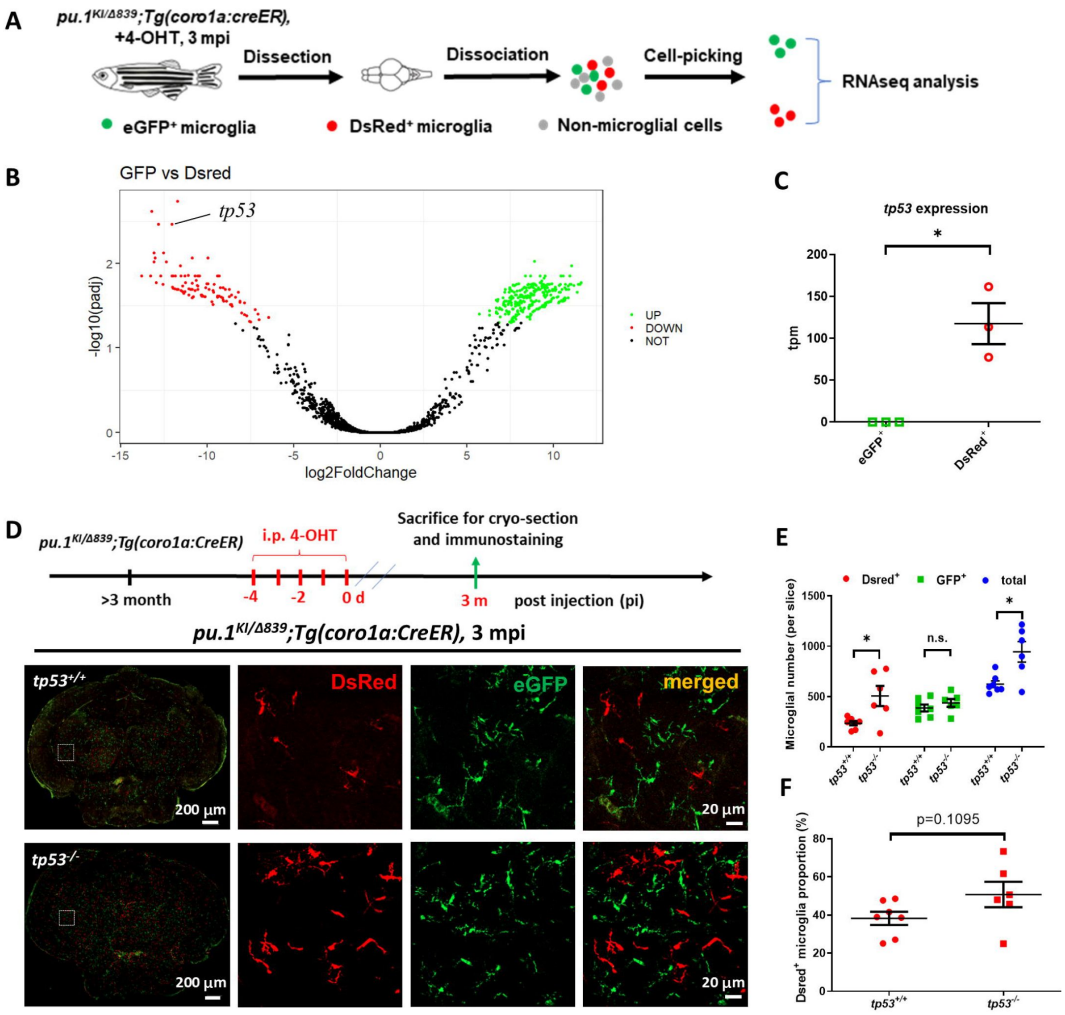

Fig. 5.

Inactivation of Tp53 largely restored the number of *pu.1*-deficient microglia in mosaic condition.

(A) The experimental setup for the isolation of eGFP$^+$ and DsRed$^+$ microglia from *pu.1$^{KI/\Delta839}$;Tg(coro1a:CreER)* adult brain at 3 mpi for transcriptomic analysis. **(B)** The volcano plot of differential expressed genes (DEG) between eGFP$^+$ and DsRed$^+$ microglia at 3 mpi. **(C)** Relative expression (tpm) of *tp53* in eGFP$^+$ (n=3) and DsRed$^+$ (n=3) microglia at 3 mpi. **(D)** The experimental setup for *pu.1* conditional knockout in wild-type and *tp53$^{-/-}$* adult zebrafish, and the representative images of midbrain cross section of *pu.1$^{KI/\Delta839}$;Tg(coro1a:CreER)* and *pu.1$^{KI/\Delta839}$;tp53$^{-/-}$;Tg(coro1a:CreER)* fish at 3 mpi. **(E)** Quantification of the number of DsRed$^+$, eGFP$^+$ and total (DsRed + eGFP) microglia in *pu.1$^{KI/\Delta839}$;Tg(coro1a:CreER)* (n=7) and *pu.1$^{KI/\Delta839}$;tp53$^{-/-}$;Tg(coro1a:CreER)* (n=6) fish at 3 mpi. **(F)** Quantification of the proportion of DsRed$^+$ microglia in *pu.1$^{KI/\Delta839}$;Tg(coro1a:CreER)* (n=7) *and pu.1$^{KI/\Delta839}$;tp53$^{-/-}$;Tg(coro1a:CreER)* (n=6) fish at 90 dpi. n.s. = not significant, p>0.05; *p<0.05.

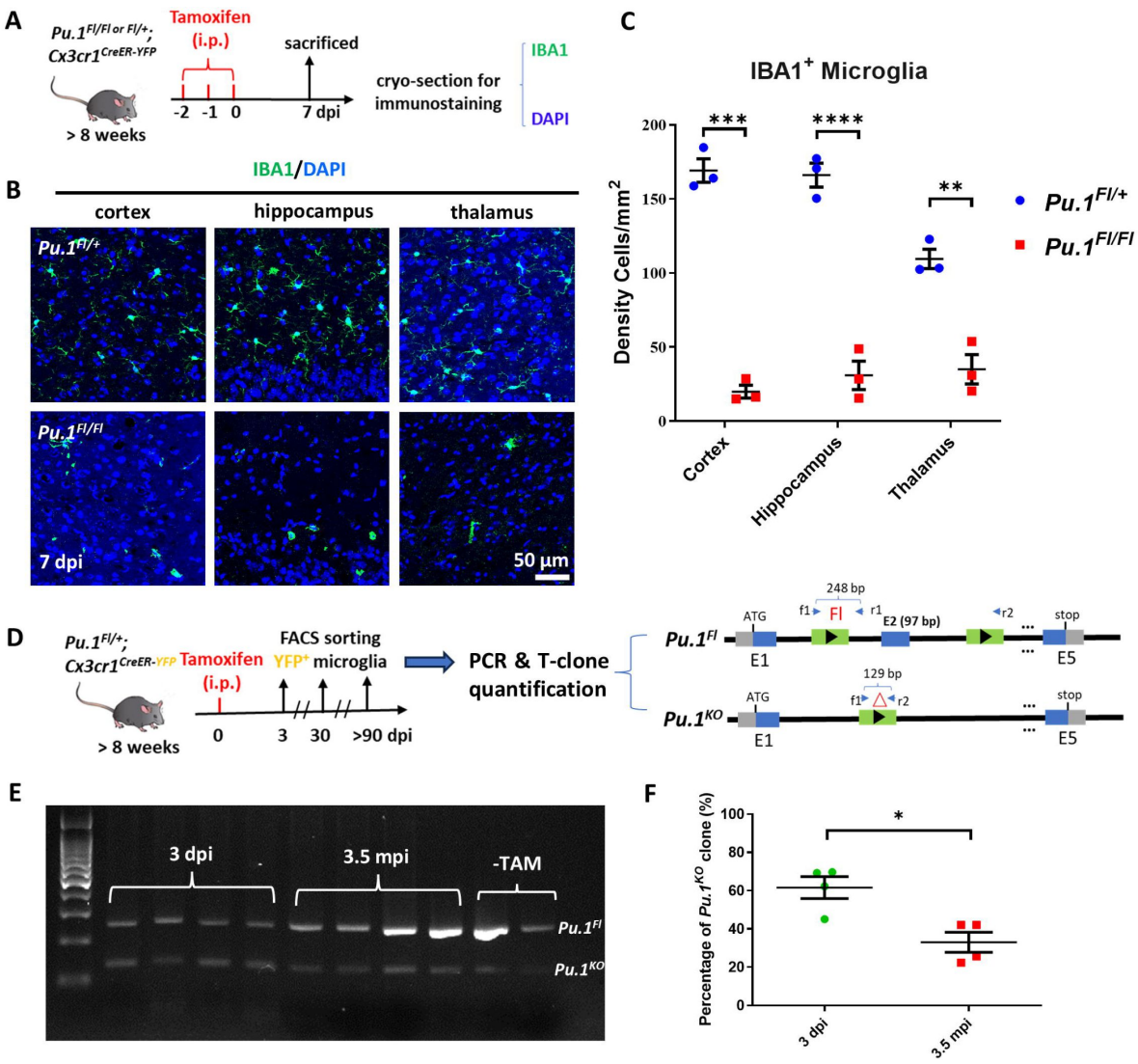

Fig. 6.

Dosage-dependent regulation of microglia maintenance by Pu.1/Spi1 is evolutionary conserved in mice.

(A) The experimental setup for *Pu.1* conditional knockout in adult mice. **(B)** Representative images of IBA1 and DAPI co-staining in the cortex, hippocampus and thalamus of $Pu.1^{Fl/+}$;$Cx3cr1^{CreER}$ and $Pu.1^{Fl/Fl}$;$Cx3cr1^{CreER}$mice at 7 dpi. **(C)** Quantification of the density of $IBA1^{+}$ microglia in the cortex, hippocampus and thalamus of $Pu.1^{Fl/+}$;$Cx3cr1^{CreER}$(n=3) and $Pu.1^{Fl/Fl}$;$Cx3cr1^{CreER}$ (n=3) mice at 7 dpi. **(D)** The experimental setup for conditional knockout of *Pu.1* in $Pu.1^{Fl/+}$;$Cx3cr1^{CreER}$ mice, and the subsequent PCR detection and T-clone quantification of $Pu.1^{Fl}$ and $Pu.1^{KO}$ alleles in sorted YFP^{+} microglia. **(E)** Gel image shows the relative intensity of amplified DNA bands of $Pu.1^{Fl}$ and $Pu.1^{KO}$alleles in microglia sorted from $Pu.1^{Fl/+}$;$Cx3cr1^{CreER}$mice at different stages post TAM injection. (**F**) Quantification of the percentage of $Pu.1^{KO}$ allele at 3 dpi (n=4) and 3.5 mpi (n=4) by T-clone assay. *p<0.05; **p<0.01; ***p<0.001; ****p<0.0001.

Discussion

In the present study, to explore the role of Pu.1 in microglia survival and maintenance, we established a visible conditional knockout *pu.1*^{KI}allele in zebrafish via the non-homologous end joining (NHEJ)-mediated knock-in method. Although conditional inactivation of targeted genes has been reported by several independent studies (Li *et al*., 2015; Li *et al*, 2019; Shin *et al*, 2023), it has not been widely applied in zebrafish, possibly due to the difficulty or low efficiency to generate loxP-flanked alleles. Compared to homologous recombination (HR), NHEJ-mediated knock-in of reporter gene has been shown to display 10-fold higher efficiency (Auer *et al*, 2014; Li *et al*., 2015). In our case, the germline transmission to F1 generation for *pu.1*^{KI} allele is around 15% (Fig. S1). Meanwhile, in our investigation, we noted that the efficiency of Cre-mediated excision of loxP sites at the *pu.1* locus in zebrafish (**Fig. 3**) appears much lower than that in mouse (**Fig. 6**). Although it remains to be further validated whether this observation is a general phenomenon, it does highlight the necessity and significance of chimera study of interested genes. In our *pu.1*^{KI}allele, the expression of DsRed directly indicates Cre-mediated excision and helps us distinguish the mutant cells from their sibling cells, which serves as a good example for chimera study in the future. Moreover, our knock-in allele can also be simply regarded as a loxP-flanked fluorescent reporter line, which not only facilitates the labeling of cells that express gene of interest, but also can be used in combination with the LEGO-IR system (Xu *et al*., 2015) to trace the fate of these cells. Thus, due to the high integration efficiency of donor DNA fragment and the multifaceted applications of the labeling strategy, we anticipated that our knock-in system would be a powerful tool and broadly be adopted in the fields of genetics, developmental biology and cell biology for the chimeric study of interested genes and fate mapping of interested cells in the future.

Via EdU pulse-chase labelling assay, we found that the daily turnover rate of microglia in adult zebrafish is about 2.5%, much higher than that reported in mice and human (Lopez-Atalaya *et al*, 2018). These disparities might be explained by several reasons. First, in our calculation of microglia turnover rate, we did not factor the unknown cell cycle length of zebrafish microglia. It is possible that the duration of microglia proliferation in zebrafish is much shorter than that in mice. If microglia proliferation takes less than 24 hours in zebrafish, then the calculated daily turnover rate of 2.5% may be overestimated. Second, it is well recognized that zebrafish manifest much stronger regeneration capability than mammals. As such, differentiated cells, like cardiomyocytes and hair cells in zebrafish are in general more proliferative than those in mammals (Chen *et al*, 2019; Marques *et al*, 2019). In this regard, microglia in zebrafish might be pre-coded both genetically and epigenetically to be more proliferative. Finally, microglia turnover could potentially be affected by the distinct efferocytotic burdens via the lysosome pathway, as lysosome has been known to be a convergent point for many biological process, including metabolism, cellular senescence, DNA repair, ER stress and even apoptosis (Franco-Juárez *et al*, 2022; Perera & Zoncu, 2016). Indeed, efferocytosis of apoptotic cells has previously been shown to elicit NOX2 assembly and promote ROS production (Yvan-Charvet *et al*, 2010), which in turn triggers cell death via induction of lysosome damage (Patra *et al*, 2023; Wang *et al*, 2018). The more regenerative environment in zebrafish might be accompanied by higher frequency of cell death, which could lead to the increase of efferocytotic burdens of microglia, thereby accelerating the turnover of microglia. Further studies will be required to clarify this issue.

Our results revealed that the survival and maintenance microglia are highly sensitive to the dosage of PU.1/SPI1 in both teleost and mammals. Interestingly, a previous study reported that hetero- or homozygosity of PU/ER(T) allele, in which the estrogen receptor (ER) ligand binding domain-G525R is fused with the full-length PU.1 to block its nucleus translocation, showed no effect on the viability of alveolar macrophages (Karpurapu *et al*., 2011). This contradictory result

might potentially result from the leakiness of ER, which was incapable to fully retain PU.1 in cytoplasm. A recent work found that conditional inactivation of PU.1 by feeding the animals with tamoxifen-containing diet in the Alzheimer's disease model CK-p25 mice led to a 33% reduction in microglia number at their young ages. Although the authors considered prevention of microgliosis as a result of the amelioration of neuroinflammation (Ralvenius *et al*., 2023), our data implies that reduction in microglia could also been interpreted by the direct involvement of PU.1 in microglia survival and maintenance, as our data clearly demonstrate that conditional ablation of the PU.1 in mice or Pu.1/Spi-b in zebrafish leads to the rapid depletion of microglia in the brain (**Fig. 6**; Fig. S4). As PU.1 is a master regulator that controls the expression of series of genes required for macrophage/microglia development (Satoh *et al*., 2014), rapid death of *Pu.1*-null microglia might probably be caused by the orchestration of multiplex factors, including the downregulation of colony-stimulating factor 1 receptor (*Csf1r*) (the essential regulator controlling the survival and maintenance of microglia in both mice and zebrafish) (Elmore *et al*., 2014; Yu *et al*., 2023), the loss of anti-apoptotic genes, such as BCL2A1 (Jenal *et al*, 2010), and absence of other genes that maintain the integrity of cells. Intriguingly, differing from the rapid death of microglia after complete inactivation of PU.1 or Pu.1/Spi-b, microglia with a partial loss of PU.1 or Pu.1 are chronically eliminated only in the mosaic condition via cell competition, in which the microglia with WT *Pu.1* or a single copy of *pu.1* are present (**Fig. 3** and **Fig. 6**). Moreover, we further showed that the chronic elimination of *pu.1*-dificent microglia in zebrafish is mediated by Tp53-dependent cell competition, which has been shown to depend on the relative level of Tp53 in competing cells (Bondar & Medzhitov, 2010; Zhang *et al*., 2017). Previously, we have shown that the level of *csf1ra*, the zebrafish orthologue of mammalian *Csf1r*, is highly associated with the fitness of microglia and regulates the turnover and maintenance of microglia via cell-competition (Yu *et al*., 2023). During the process of investigation, we also wondered whether the cell competition between *pu.1*-deficient microglia and *pu.1*-sufficient microglia relied on Csf1ra. However, in contrast to the robust upregulation of *p53* in *pu.1*-deficient microglia, the decrease of *csf1ra* was not observed (Fig. S9). In summary, our findings suggest that the dosage of PU.1/Pu.1 may serve as a checkpoint to determine the fitness of microglia. It will be of great interest to explore the upstream events that modulate *PU.1*/*pu.1* expression during microglia turnover.

Materials and Methods

Zebrafish

Zebrafish were maintained according to standard protocol as described previously (Westerfield, 2000). AB wild-type, $pu.1^{\Delta 839}$ (Yu *et al*., 2017), $spi\text{-}b^{\Delta 232}$ (Yu *et al*., 2017), $tp53^{M214K}$ (Berghmans *et al*, 2005), $pu.1^{KI}$ (short for $pu.1^{KI}$-eGFP), $pu.1^{CKO}$ (short for $pu.1^{KI}$-DsRed), *TgBAC(ccl34b.1:eGFP)* (Wu *et al*., 2020), $Tg(coro1a{:}CreER^{T2})^{sz101tg}$, *Tg(mpeg1:loxP-DsRedx-loxP-eGFP, shorted as LRLG)*^{hkz015t} (Xu *et al*, 2016) were used in this study.

Mouse strains

$Pu.1^{Fl}$ (No.T010980, purchased from GemPharmatech Co.,Ltd) and $Cx3cr1^{CreER\text{-}EYFP}$ (Stock No. 021160) (Yona *et al*., 2013) were used in this study. All animal experiments and procedures were proved by Ethics Committee for the Welfare of Laboratory Animals in Shenzhen PKU-HKUST Medical Center.

Generation of $pu.1^{KI}$ allele

Donor plasmid was modified based on the reported Th-KI plasmid (Li *et al*., 2015). In brief, DNA fragments containing *pu.1* exon 4 to exon 6 and the 3' downstream fragment were cloned from cDNA and genomic DNA libraries respectively and inserted into the plasmid containing P2A-eGFP, P2A-Dsred and loxP elements. sgRNA was designed in the intron 3~4 of *pu.1* with the online website Crisprscan (*https://www.crisprscan.org/*). It was transcribed by MEGAshortscript Kit

(AM1354, Invitrogen) from PCR product which was amplified following reported protocol (Vejnar *et al*, 2016). Then Cas9 mRNA (700 ng/ul), sgRNA (70 ng/ul) and donor plasmid (15 ng/ul) were mixed and injected into zebrafish embryos at one-cell stage. Embryos with eGFP signal were selected at 3 dpf and raised to adulthood for germline transmission. Adult F0 fish were crossed with wild-type fish to generate F1 and $eGFP^{+}$ F1 were selected. The 5'- and 3'-junctions of the donor plasmid integration site were amplified from the genomic DNA of F1 embryos and sent for sequencing. The primers used for 5' junction are 5'-GATCTATCGACCACCAATGGAG-3' and 5'-GCCATAGTGTGCATTCTCAGG-3' and for 3' junction are 5'-GTTGTAAAACGACGGCCAG-3' and 5'-GAGTGTAGTGCTCATTCAAGC-3'.

Cryo-section

Adult fish were anesthetized on ice. The tissue was dissected and fixed in 4% PFA at 4 [overnight. After being washed with phosphate-buffered saline (PBS) at room temperature for 1 day, the tissues were dehydrated with 30% sucrose at 4 [overnight, then soaked in coagulating solution (optimal cutting temperature compound, OCT) and subjected to cryosection with 30-μm thickness.

EdU and BrdU incorporation assays, TUNEL staining, and immunostaining

EdU and BrdU incorporation assays were conducted as previously reported (Yu *et al*., 2023). In brief, EdU (A10044, Invitrogen) or BrdU (B5002, Sigma-Aldrich) was dissolved in PBS to the final concentration of 10 mg/ml. 5 ul EdU or BrdU was intraperitoneally (i.p.) injected into adult zebrafish each time. Brain samples were dissected at 1 day post injection and fixed in 4% PFA for cryosection.

EdU detection was conducted with (Click-iT™ EdU Cell Proliferation Kit for Imaging, Alexa Fluor™ 647 dye, Invitrogen, C10340) according to the manufacturer's instructions. For BrdU detection, samples were treated with 2M HCl for half an hour and then stained with the BrdU antibody. TUNEL staining was performed with TUNEL BrightGreen Apoptosis Detection Kit (A112, Vazyme) according to the manufacturer's instructions. Antibody staining was performed after EdU/BrdU and TUNEL detection. Primary antibodies used in this study were mouse anti-BrdU (11170376001, Roche), goat anti-GFP (ab6658, Abcam), rabbit anti-DsRed (632496, Clontech), rabbit anti-Lcp1 (Jin *et al*, 2009), rabbit anti-Pu.1 (Jin *et al*, 2012) and rabbit anti-IBA1 (019-19741, FUJIFILM Wako) antibodies.

Tamoxifen injection

4-Hydroxytamoxifen (4-OHT, H7904, Sigma) was dissolved in ethanol to final concentration of 10 mM. For adult fish, 1 ul 4-OHT was i.p. injected into each fish for 3 times. For adult mice, tamoxifen (T5648, Sigma) was dissolved in corn oil to final concentration of 20 mg/ml and i.p. injected into the mice with 35 mg/kg (sub-dosage) or 150 mg/kg (over-dosage).

Neutral red staining

Neutral red staining was performed as previously described (Herbomel *et al*, 2001).

Cy5-Annexin V treatment

Annexin V-Cy5 Reagent (1013, Biovision) solution was directly injected into brain ventricle of 3 dpf larva and immediately imaged by confocal microscope.

Imaging

Fluorescent signals from live reporter lines or immunostaining were imaged under a Leica SP8 confocal microscope or a Zeiss LSM980 confocal microscope. The objectives HC PL APO 203/0.70 DRY (Leica) and Plan-Apochromat 20×/0.8 M27 (Zeiss) were used in this study.

cDNA preparation and RNA-seq

Cell suspensions were prepared as previously described (Yu *et al*., 2017). Cells of interest were manually picked under the fluorescent microscope (Nikon Ti-S) equipped with the micro-manipulator (NT-88-V3, Nikon). Subsequently, picked cells were transferred by the glass needle to lysis buffer (mainly including Triton X-100 and RNase inhibitor) for thorough vertex. Then the cell lysate was used for reverse-transcription and amplification with the Smart-Seq2 method (Picelli *et al*, 2014) to generate the cDNA library. cDNA was sent to Novogene Company for Illumina sequencing with an average depth of 6×10^6 raw reads per sample. Sequence data were aligned to zebrafish genome by STAR (Spliced Transcripts Alignment to a Reference). Samples with strong expression of microglia-related genes and faint DC-related genes were chosen for further analysis.

Mouse microglia isolation

Adult mice brain was dissected and cut into small pieces. They were dissociated into single-cell suspensions with Adult Brain Dissociation Kit (130-107-677, Miltenyi Biotec) according to the manufacturer's instructions. Then Myelin Removal Beads II (130-96-733, Miltenyi Biotec) were used to remove myelin debris from single-cell suspensions. YFP^+ Microglia were sorted from suspensions by FACS Aria IIIu. The sorted microglia were lysed by proteinase K to extract DNA or TRIzol to extract RNA.

TA clone assay

$Pu.1^{Fl}$ and $Pu.1^{KO}$ alleles were amplified by PCR from the genomic DNA. The common forward primer was 5'-GCATCGCATTGTCTGAGTAGGT-3. The reverse primers were 5'-AAATCTGCCTGGGTGACCTTC-3' for $Pu.1^{Fl}$ and 5'-ACACAACGGGTTCTTCTGTTAG-3' for $Pu.1^{KO}$. The PCR products for $Pu.1^{Fl}$ and $Pu.1^{KO}$ alleles were 248 bp and 129 bp respectively. PCR products were ligated to pUCm-T vector (B522211, Sangon) with Blunt/TA Ligase Master Mix (M0367S, NEB) according to the manufacturer's instructions. The clones containing ligated plasmids were amplified with M13F (5'-GTTGTAAAACGACGGCCAG-3') and M13R (5'-CAGGAAACAGCTATGAC-3'). The PCR products for $Pu.1^{Fl}$ and $Pu.1^{KO}$ alleles were 437 bp and 315 bp respectively. Clones of $Pu.1^{Fl}$ and $Pu.1^{KO}$ alleles were distinguished by the size of PCR products.

Quantitative PCR

cDNA was synthesized from extracted RNA with SuperScript™ III Reverse Transcriptase kit (18080093, Invitrogen). Quantitative PCR was performed with iTaq™ Universal SYBR® Green Supermix (1725121, Bio-rad) on a CFX96 Dx Instrument (Bio-rad) and analyzed using the ΔΔCt method. The following primers were used to determine the expression of *DsRed* and *pu.1* from $pu.1^{CKO}$allele: *DsRed*, 5'-GATCTATCGACCACCAATGGAG-3' (*pu.1*-161FP)/ 5'-GCCGTTCACGGAGCCCTCCAT-3' (DsRed-72RP); *pu.1*, 5'-GATCTATCGACCACCAATGGAG-3' (*pu.1*-161FP)/ 5'-CGCATGTAGTGACTGCACGC-3' (*pu.1*-357RP). The following primers were used to determine the expression of *Pu.1* and *Spi-b* in mouse microglia: *Gapdh*, 5'-TGTGTCCGTCGTGGATCTGA-3'/5'-TTGCTGTTGAAGTCGCAGGAG-3'; *Pu.1*, 5'-GAGGTGTCTGATGGAGAAGCTG-3'/5'-ACCCACCAGATGCTGTCCTTCA-3'; *Spi-b*, 5'-AGGAGTCTTCTACGACCTGGAC-3'/5'-GGAGTGGCTAAAGGCAGCAGTA-3'.

Quantification and Statistics

The number microglia in embryos were quantified manually, and then genotyped to prevent bias. For the experiment with adults, fish were genotyped first and then numbered without gender bias for downstream 4-OHT injection, brain sample collection, cryo-section and immunostaining experiments. For microglia number quantification, 3 representative slices from anterior, middle and posterior of the midbrain of numbered fish were chosen for further manual counting with the same criterial. For EdU/BrdU or TUNEL experiments, at least 6 representative slices from anterior, middle and posterior of the midbrain were chosen for calculation. The number of EdU/BrdU^{+} or TUNEL^{+} microglia/DCs from the slices were counted and then divided by the total number of microglia/DCs to calculate the ratio.

Adult mice were genotyped first and then only males were chosen for the downstream experiments. For statistics, cortex, hippocampus and thalamus on the slices of mouse brain were chosen for microglia density quantification. The number of microglia and region of interest were calculated with Imaris 9.9 software to determine the density.

Statistical analyses are performed with Graphpad Prism 9.5.1. F test was first used to check the variances of two groups. If the variances of two groups were not significantly different ($P>0.05$), Student's t test was performed. If the variances of the two groups were significantly different ($P<0.05$), t test with Welch's correction was performed. A result was considered significant if $P<0.05$. Values represent mean ± standard error of the mean.

Acknowledgements

We thank Dr. Keng Chen and Dr. Keyu Chen in Shenzhen Bay Laboratory for their assistance in the Fluorescent-activated cell sorting (FACS) of mouse microglia, and thank Prof. Jin Xu in South China University of Technology for his kind suggestions on this project.

Additional information

Funding

This work is supported by National Natural Science Foundation of China Grant (31801211), Natural Science Foundation of Guangdong Province Grant (2024A1515030122), Shenzhen Medical Academy of Research and Translation (SMART) 2023 Shenzhen Medical Research Funding (B2302034), and Research Grants Council of the Hong Kong Special Administrative Region Grants (16103920, AoE/M-09/12, T13-605/18-W, and T13-602/21-N).

Additional files

Supplemental Figure 1-9

References

1. Ajami B, Bennett JL, Krieger C, Tetzlaff W, Rossi FMV 2007) **Local self-renewal can sustain CNS microglia maintenance and function throughout adult life** *Nature neuroscience* **10**:1538–1543

2. Askew K, Li K, Olmos-Alonso A, Garcia-Moreno F, Liang Y, Richardson P, Tipton T, Chapman MA, Riecken K, Beccari S, et al 2017) **Coupled Proliferation and Apoptosis Maintain the Rapid Turnover of Microglia in the Adult Brain** *Cell Rep* **18**:391–405

3. Auer TO, Duroure K, De Cian A, Concordet JP, Del Bene F 2014) **Highly efficient CRISPR/Cas9-mediated knock-in in zebrafish by homology-independent DNA repair** *Genome research* **24**:142–153

4. Berghmans S, Murphey RD, Wienholds E, Neuberg D, Kutok JL, Fletcher CDM, Morris JP, Liu TX, Schulte-Merker S, Kanki JP, et al 2005) **tp53 mutant zebrafish develop malignant peripheral nerve sheath tumors** *Proceedings of the National Academy of Sciences* **102**:407–412

5. Bondar T, Medzhitov R 2010) **p53-Mediated Hematopoietic Stem and Progenitor Cell Competition** *Cell Stem Cell* **6**:309–322

6. Bruttger J, Karram K, Wörtge S, Regen T, Marini F, Hoppmann N, Klein M, Blank T, Yona S, Wolf Y, et al 2015) **Genetic Cell Ablation Reveals Clusters of Local Self-Renewing Microglia in the Mammalian Central Nervous System** *Immunity* **43**:92–106

7. Cao H, Zhou X, Chen Y, Ip FCF, Chen Y, Lai NCH, Lo RMN, Tong EPS, Mok VCT, Kwok TCY, et al 2022) **Association of SPI1 Haplotypes with Altered SPI1 Gene Expression and Alzheimer's Disease Risk** *J Alzheimers Dis* **86**:1861–1873

8. Chen Y, Zhang S, Chai R, Li H, Li H., Chai R. 2019) **Hair Cell Regeneration** In: *Hearing Loss: Mechanisms, Prevention and Cure* Singapore: Springer Singapore pp. 1–16

9. Colonna M, Butovsky O 2017) **Microglia Function in the Central Nervous System During Health and Neurodegeneration** *Annual Review of Immunology* **35**:441–468

10. Monica RP Elmore, Allison R Najafi, Maya A Koike, Nabil N Dagher, Elizabeth E Spangenberg, Rachel A Rice, Kitazawa M, Matusow B, Nguyen H, West Brian L, Green Kim N 2014) **Colony-Stimulating Factor 1 Receptor Signaling Is Necessary for Microglia Viability, Unmasking a Microglia Progenitor Cell in the Adult Brain** *Neuron* **82**:380–397

11. Franco-Juárez B, Coronel-Cruz C, Hernández-Ochoa B, Gómez-Manzo S, Cárdenas-Rodríguez N, Arreguin-Espinosa R, Bandala C, Canseco-Ávila LM, Ortega-Cuellar D 2022) **TFEB; Beyond Its Role as an Autophagy and Lysosomes Regulator** *Cells* **11**:3153

12. Füger P, Hefendehl JK, Veeraraghavalu K, Wendeln AC, Schlosser C, Obermüller U, Wegenast-Braun BM, Neher JJ, Martus P, Kohsaka S, et al 2017) **Microglia turnover with aging and in an Alzheimer's model via long-term in vivo single-cell imaging** *Nature neuroscience* **20**:1371–1376

13. Ginhoux F, Greter M, Leboeuf M, Nandi S, See P, Gokhan S, Mehler MF, Conway SJ, Ng LG, Stanley ER, et al 2010) **Fate mapping analysis reveals that adult microglia derive from primitive macrophages** *Science* **330**:841–845

14. Glass CK, Saijo K, Winner B, Marchetto MC, Gage FH 2010) **Mechanisms underlying inflammation in neurodegeneration** *Cell* **140**:918–934

15. Gomez-Nicola D, Perry VH 2015) **Microglial Dynamics and Role in the Healthy and Diseased Brain: A Paradigm of Functional Plasticity** *The Neuroscientist* **21**:169–184

16. Herbomel P, Thisse B, Thisse C 2001) **Zebrafish early macrophages colonize cephalic mesenchyme and developing brain, retina, and epidermis through a M-CSF receptor-dependent invasive process** *Developmental biology* **238**:274–288

17. Huang KL, Marcora E, Pimenova AA, Di Narzo AF, Kapoor M, Jin SC, Harari O, Bertelsen S, Fairfax BP, Czajkowski J, et al 2017) **A common haplotype lowers PU.1 expression in myeloid cells and delays onset of Alzheimer's disease** *Nature neuroscience* **20**:1052–1061

18. Hughes AN, Appel B 2020) **Microglia phagocytose myelin sheaths to modify developmental myelination** *Nature neuroscience* **23**:1055–1066

19. Iyer H, Shen K, Meireles AM, Talbot WS 2022) **A lysosomal regulatory circuit essential for the development and function of microglia** *Sci Adv* **8**:eabp8321

20. Jenal M, Batliner J, Reddy VA, Haferlach T, Tobler A, Fey MF, Torbett BE, Tschan MP 2010) **The anti-apoptotic gene BCL2A1 is a novel transcriptional target of PU.1** *Leukemia* **24**:1073–1076

21. Jin H, Li L, Xu J, Zhen F, Zhu L, Liu PP, Zhang M, Zhang W, Wen Z 2012) **Runx1 regulates embryonic myeloid fate choice in zebrafish through a negative feedback loop inhibiting Pu.1 expression** *Blood* **119**:5239–5249

22. Jin H, Sood R, Xu J, Zhen F, English MA, Liu PP, Wen Z 2009) **Definitive hematopoietic stem/progenitor cells manifest distinct differentiation output in the zebrafish VDA and PBI** *Development* **136**:647–654

23. Karpurapu M, Wang X, Deng J, Park H, Xiao L, Sadikot RT, Frey RS, Maus UA, Park GY, Scott EW, Christman JW 2011) **Functional PU.1 in macrophages has a pivotal role in NF-κB activation and neutrophilic lung inflammation during endotoxemia** *Blood* **118**:5255–5266

24. Kierdorf K, Erny D, Goldmann T, Sander V, Schulz C, Perdiguero EG, Wieghofer P, Heinrich A, Riemke P, Holscher C, et al 2013) **Microglia emerge from erythromyeloid precursors via Pu.1- and Irf8-dependent pathways** *Nature neuroscience* **16**:273–280

25. Lawson LJ, Perry VH, Gordon S 1992) **Turnover of resident microglia in the normal adult mouse brain** *Neuroscience* **48**:405–415

26. Li J, Zhang BB, Ren YG, Gu SY, Xiang YH, Du JL 2015) **Intron targeting-mediated and endogenous gene integrity-maintaining knockin in zebrafish using the CRISPR/Cas9 system** *Cell research* **25**:634–637

27. Li W, Zhang Y, Han B, Li L, Li M, Lu X, Chen C, Lu M, Zhang Y, Jia X, et al 2019) **One-step efficient generation of dual-function conditional knockout and geno-tagging alleles in zebrafish** *eLife* :8

28. Li Y, Du X-f, Liu C-s, Wen Z-l, Du J-l 2012) **Reciprocal Regulation between Resting Microglial Dynamics and Neuronal Activity In Vivo** *Developmental cell* **23**:1189–1202

29. Lopez-Atalaya JP, Askew KE, Sierra A, Gomez-Nicola D 2018) **Development and maintenance of the brain's immune toolkit: Microglia and non-parenchymal brain macrophages** *Dev Neurobiol* **78**:561–579

30. Marques IJ, Lupi E, Mercader N 2019) **Model systems for regeneration: zebrafish** *Development* :146

31. McKercher SR, Torbett BE, Anderson KL, Henkel GW, Vestal DJ, Baribault H, Klemsz M, Feeney AJ, Wu GE, Paige CJ, Maki RA 1996) **Targeted disruption of the PU.1 gene results in multiple hematopoietic abnormalities** *The EMBO journal* **15**:5647–5658

32. Ou H-L, Schumacher B 2018) **DNA damage responses and p53 in the aging process** *Blood* **131**:488–495

33. Patra S, Patil S, Klionsky DJ, Bhutia SK 2023) **Lysosome signaling in cell survival and programmed cell death for cellular homeostasis** *Journal of Cellular Physiology* **238**:287–305

34. Perera RM, Zoncu R 2016) **The Lysosome as a Regulatory Hub** *Annual Review of Cell and Developmental Biology* **32**:223–253

35. Peri F, Nüsslein-Volhard C 2008) **Live Imaging of Neuronal Degradation by Microglia Reveals a Role for v0-ATPase a1 in Phagosomal Fusion In Vivo** *Cell* **133**:916–927

36. Picelli S, Faridani OR, Björklund ÅK, Winberg G, Sagasser S, Sandberg R 2014) **Full-length RNA-seq from single cells using Smart-seq2** *Nature Protocols* **9**:171

37. Prinz M, Priller J, Sisodia SS, Ransohoff RM 2011) **Heterogeneity of CNS myeloid cells and their roles in neurodegeneration** *Nature neuroscience* **14**:1227–1235

38. Ralvenius WT, Mungenast AE, Woolf H, Huston MM, Gillingham TZ, Godin SK, Penney J, Cam HP, Gao F, Fernandez CG, et al 2023) **A novel molecular class that recruits HDAC/MECP2 complexes to PU.1 motifs reduces neuroinflammation** *J Exp Med* **220**

39. Satoh J, Asahina N, Kitano S, Kino Y 2014) **A Comprehensive Profile of ChIP-Seq-Based PU.1/Spi1 Target Genes in Microglia** *Gene Regul Syst Bio* **8**:127–139

40. Schulz C, Gomez Perdiguero E, Chorro L, Szabo-Rogers H, Cagnard N, Kierdorf K, Prinz M, Wu B, Jacobsen SE, Pollard JW, et al 2012) **A lineage of myeloid cells independent of Myb and hematopoietic stem cells** *Science* **336**:86–90

41. Scott EW, Simon MC, Anastasi J, Singh H 1994) **Requirement of transcription factor PU.1 in the development of multiple hematopoietic lineages** *Science* **265**:1573–1577

42. Shin M, Yin HM, Shih YH, Nozaki T, Portman D, Toles B, Kolb A, Luk K, Isogai S, Ishida K, et al 2023) **Generation and application of endogenously floxed alleles for cell-specific knockout in zebrafish** *Developmental cell* **58**:2614–2626

43. Smith AM, Gibbons HM, Oldfield RL, Bergin PM, Mee EW, Faull RL, Dragunow M 2013) **The transcription factor PU.1 is critical for viability and function of human brain microglia** *Glia* **61**:929–942

44. Su GH, Chen HM, Muthusamy N, Garrett-Sinha LA, Baunoch D, Tenen DG, Simon MC 1997) **Defective B cell receptor-mediated responses in mice lacking the Ets protein, Spi-B** *The EMBO journal* **16**:7118–7129

45. Tay TL, Mai D, Dautzenberg J, Fernández-Klett F, Lin G, Sagar Datta M, Drougard A, Stempfl T, Ardura-Fabregat A, et al 2017) **A new fate mapping system reveals context-dependent random or clonal expansion of microglia** *Nature neuroscience* **20**:793–803

46. Vaddavalli PL, Schumacher B 2022) **The p53 network: cellular and systemic DNA damage responses in cancer and aging** *Trends in Genetics* **38**:598–612

47. Vejnar CE, Moreno-Mateos MA, Cifuentes D, Bazzini AA, Giraldez AJ 2016) **Optimized CRISPR-Cas9 System for Genome Editing in Zebrafish** *Cold Spring Harb Protoc* :2016

48. Walton MR, Gibbons H, MacGibbon GA, Sirimanne E, Saura J, Gluckman PD, Dragunow M 2000) **PU.1 expression in microglia** *J Neuroimmunol* **104**:109–115

49. Wang F, Gómez-Sintes R, Boya P 2018) **Lysosomal membrane permeabilization and cell death** *Traffic* **19**:918–931

50. Westerfield M 2000) **The Zebrafish Book: A Guide for the Laboratory Use of Zebrafish (Danio rerio)** Eugene: University of Oregon Press

51. Wu S, Nguyen LTM, Pan H, Hassan S, Dai Y, Xu J, Wen Z 2020) **Two phenotypically and functionally distinct microglial populations in adult zebrafish** *Sci Adv* :6

52. Xu J, Wang T, Wu Y, Jin W, Wen Z 2016) **Microglia Colonization of Developing Zebrafish Midbrain Is Promoted by Apoptotic Neuron and Lysophosphatidylcholine** *Developmental cell* **38**:214–222

53. Xu J, Zhu L, He S, Wu Y, Jin W, Yu T, Qu JY, Wen Z 2015) **Temporal-Spatial Resolution Fate Mapping Reveals Distinct Origins for Embryonic and Adult Microglia in Zebrafish** *Developmental cell* **34**:632–641

54. Yona S, Kim K-W, Wolf Y, Mildner A, Varol D, Breker M, Strauss-Ayali D, Viukov S, Guilliams M, Misharin A, et al 2013) **Fate Mapping Reveals Origins and Dynamics of Monocytes and Tissue Macrophages under Homeostasis** *Immunity* **38**:79–91

55. Yu T, Guo W, Tian Y, Xu J, Chen J, Li L, Wen Z 2017) **Distinct regulatory networks control the development of macrophages of different origins in zebrafish** *Blood* **129**:509–519

56. Yu T, Kuang H, Wu X, Huang Y, Wang J, Wen Z 2023) **Cell competition for neuron-derived trophic factor controls the turnover and lifespan of microglia** *Sci Adv* **9**:eadf9790

57. Yvan-Charvet L, Pagler TA, Seimon TA, Thorp E, Welch CL, Witztum JL, Tabas I, Tall AR 2010) **ABCA1 and ABCG1 Protect Against Oxidative Stress–Induced Macrophage Apoptosis During Efferocytosis** *Circulation Research* **106**:1861–1869

58. Zhang G, Xie Y, Zhou Y, Xiang C, Chen L, Zhang C, Hou X, Chen J, Zong H, Liu G 2017) **p53 pathway is involved in cell competition during mouse embryogenesis** *Proceedings of the National Academy of Sciences* **114**:498–503

59. Zhou Q, Zhao C, Yang Z, Qu R, Li Y, Fan Y, Tang J, Xie T, Wen Z 2023) **Cross-organ single-cell transcriptome profiling reveals macrophage and dendritic cell heterogeneity in zebrafish**

Author information

Yi Wu[#]
Biomedical Research Institute, Shenzhen Peking University-the Hong Kong University of Science and Technology Medical Center, Shenzhen, China

[#]These authors contribute equally to this work.

Weilin Guo[#]
Division of Life Science, the Hong Kong University of Science and Technology, Hong Kong, China

[#]These authors contribute equally to this work.

Haoyue Kuang
Greater Bay Biomedical Innocenter, Shenzhen Bay Laboratory, Shenzhen, China

Xiaohai Wu
Greater Bay Biomedical Innocenter, Shenzhen Bay Laboratory, Shenzhen, China

Yuexin Wang
Greater Bay Biomedical Innocenter, Shenzhen Bay Laboratory, Shenzhen, China

Shizheng Zhao
Biomedical Research Institute, Shenzhen Peking University-the Hong Kong University of Science and Technology Medical Center, Shenzhen, China

Zilong Wen
Division of Life Science, the Hong Kong University of Science and Technology, Hong Kong, China, Greater Bay Biomedical Innocenter, Shenzhen Bay Laboratory, Shenzhen, China

Tao Yu
Biomedical Research Institute, Shenzhen Peking University-the Hong Kong University of Science and Technology Medical Center, Shenzhen, China, Greater Bay Biomedical Innocenter, Shenzhen Bay Laboratory, Shenzhen, China

For correspondence: tyu@connect.ust.hk

Editors

Reviewing Editor
Harini Iyer
Howard Hughes Medical Institute, University of Illinois at Urbana-Champaign, Urbana, United States of America

Senior Editor
Didier Stainier
Max Planck Institute for Heart and Lung Research, Bad Nauheim, Germany

Reviewer #1 (Public review):

Summary:

The article entitled "Pu.1/Spi1 dosage controls the turnover and maintenance of microglia in zebrafish and mammals" by Wu et al., identifies a role for the master myeloid developmental regulator Pu.1 in the maintenance of microglial populations in the adult. Using a non-homologous end joining knock-in strategy, the authors generated a pu.1 conditional allele in zebrafish, which reports wildtype expression of pu.1 with EGFP and truncated expression of pu.1 with DsRed after Cre-mediated recombination. When crossed to existing pu.1 and spi-b mutants, this approach allowed the authors to target a single allele for recombination and induce homozygous loss-of-function microglia in adults. This identified that although there is no short-term consequence to loss of pu.1, microglia lacking any functional copy of pu.1 are depleted over the course of months, even when spi-b is fully functional. The authors go on to identify reduced proliferation, increased cell death, and higher expression of tp53 in the pu.1 deficient microglia, as compared to the wild-type EGFP+ microglia. To extend these findings to mammals, the authors generated a conditional Pu.1 allele in mice and performed similar analyses, finding that loss of a single copy of Pu.1 resulted in similar long-term loss of Pu.1-deficient microglia. The conclusions of this paper are overall well supported by the data.

Strengths:

The genetic approaches here for visualizing the recombination status of an endogenous allele are very clever, and by comparing the turnover of wildtype and mutant cells in the same animal the authors can make very convincing arguments about the effect of chronic loss of pu.1. Likely this phenotype would be either very subtle or nonexistent without the point of comparison and competition with the wildtype cells.

Using multiple species allows for more generalizable results, and shows conservation of the phenomena at play.

The demonstration of changes to proliferation and cell death in concert with higher expression of tp53 is compelling evidence for the authors' argument.

Weaknesses:

This paper is very strong. It would benefit from further investigating the specific relationship between pu.1 and tp53 specifically. Does pu.1 interact with the tp53 locus? Specific molecular analysis of this interaction would strengthen the mechanistic findings.

https://doi.org/10.7554/eLife.105788.1.sa2

Reviewer #2 (Public review):

Summary:

In the presented work by Wu et al, the authors investigate the role of the transcription factor Pu.1 in the survival and maintenance of microglia, the tissue-resident macrophage population in the brain. To this end, they generated a sophisticated new conditional pu.1 allele in zebrafish using CRISPR-mediated genome editing which allows visual detection of expression of the mutant allele through a switch from GFP to dsRed after Cre-mediated recombination. Using EdU pulse-chase labelling, they first estimated the daily turnover rate

of microglia in the adult zebrafish brain which was found to be higher than rates previously estimated for mice and humans. After conditional deletion of pu.1 in coro1a positive cells, they do not find a difference in microglia number at 2 and 8 days or 1-month post-injection of Tamoxifen. However, at 3 months post-injection, a strong decrease in mutant microglia could be detected. While no change in microglia number was detected at 1mpi, an increase in apoptotic cells and decreased proliferation as observed. RNA-seq analysis of WT and mutant microglia revealed an upregulation of tp53, which was shown to play a role in the depletion of pu.1 mutant microglia as deletion in tp53-/- mutants did not lead to a decrease in microglia number at 3mpi. Through analysis of microglia number in pU.1 mutants, the authors further show that the depletion of microglia in the conditional mutants is dependent on the presence of WT microglia. To show that the phenomenon is conserved between species, similar experiments were also performed in mice.

This work expands on previous in vitro studies using primary human microglia. The majority of conclusions are well supported by the data, addition of controls and experimental details would strengthen the conclusions and rigor of the paper.

Strengths:

Generation of an elegantly designed conditional pu.1 allele in zebrafish that allows for the visual detection of expression of the knockout allele.

The combination of analysis of pu.1 function in two model systems, zebrafish and mouse, strengthens the conclusions of the paper.

Confirmation of the functional significance of the observed upregulation of tp53 in mutant microglia through double mutant analysis provides some mechanistic insight.

Weaknesses:

(1) The presented RNA-Seq analysis of mutant microglia is underpowered and details on how the data was analyzed are missing. Only 9-15 cells were analyzed in total (3 pools of 3-5 cells each). Further, the variability in relative gene expression of ccl35b.1, which was used as a quality control and inclusion criterion to define pools consisting of microglia, is extremely high (between ~4 and ~1600, Figure S7A).

(2) The authors conclude that the reduction of microglia observed in the adult brain after cKO of pu.1 in the spi-b mutant background is due to apoptosis (Lines 213-215). However, they only provide evidence of apoptosis in 3-5 dpf embryos, a stage at which loss of pu.1 alone does lead to a complete loss of microglia (Figure 2E). A control of pu.1 KI/d839 mutants treated with 4-OHT should be added to show that this effect is indeed dependent on the loss of spi-b. In addition, experiments should be performed to show apoptosis in the adult brain after cKO of pu.1 in spi-b mutants as there seems to be a difference in the requirement of pu.1 in embryonic and adult stages.

(3) The number of microglia after pu.1 knockout in zebrafish did only show a significant decrease 3 months after 4-OHT injection, whereas microglia were almost completely depleted already 7 days after injection in mice. This major difference is not discussed in the paper.

(4) Data is represented as mean +/-.SEM. Instead of SEM, standard deviation should be shown in all graphs to show the variability of the data. This is especially important for all graphs where individual data points are not shown. It should also be stated in the figure legend if SEM or SD is shown.

https://doi.org/10.7554/eLife.105788.1.sa1

Author response:

> ***Reviewer #1 (Public review):***
>
> *Strengths:*
>
> *The genetic approaches here for visualizing the recombination status of an endogenous allele are very clever, and by comparing the turnover of wildtype and mutant cells in the same animal the authors can make very convincing arguments about the effect of chronic loss of pu.1. Likely this phenotype would be either very subtle or nonexistent without the point of comparison and competition with the wildtype cells.*
>
> *Using multiple species allows for more generalizable results, and shows conservation of the phenomena at play.*
>
> *The demonstration of changes to proliferation and cell death in concert with higher expression of tp53 is compelling evidence for the authors' argument.*
>
> *Weaknesses:*
>
> *This paper is very strong. It would benefit from further investigating the specific relationship between pu.1 and tp53 specifically. Does pu.1 interact with the tp53 locus? Specific molecular analysis of this interaction would strengthen the mechanistic findings.*

We agree with the reviewer's assessment regarding the significance of the relationship between PU.1 and TP53. A previous study by Tschan et al(1) has shown that PU.1 attenuates the transcriptional activity of the *p53* tumor suppressor family through direct binding to the DNA-binding and/or the oligomerization domains of p53/p73 proteins. We will discuss this point in the revised manuscript and cite this paper accordingly. Moreover, to further investigate the interaction between Pu.1 and Tp53 in zebrafish, we intend to perform a comprehensive analysis of the *tp53* promoter region utilizing bioinformatic prediction tools. This approach aims to identify potential Pu.1 binding sites, thereby providing insights into the direct regulatory interactions between Pu.1 and the *tp53* promoter in zebrafish.

> ***Reviewer #2 (Public review):***
>
> *Strengths:*
>
> *Generation of an elegantly designed conditional pu.1 allele in zebrafish that allows for the visual detection of expression of the knockout allele.*
>
> *The combination of analysis of pu.1 function in two model systems, zebrafish and mouse, strengthens the conclusions of the paper.*
>
> *Confirmation of the functional significance of the observed upregulation of tp53 in mutant microglia through double mutant analysis provides some mechanistic insight.*
>
> *Weaknesses:*
>
> *(1) The presented RNA-Seq analysis of mutant microglia is underpowered and details on how the data was analyzed are missing. Only 9-15 cells were analyzed in total (3 pools of 3-5 cells each). Further, the variability in relative gene expression of ccl35b.1, which was used as a quality control and inclusion criterion to define pools consisting of microglia, is extremely high (between ~4 and ~1600, Figure S7A).*

In the revised manuscript, we will elaborate on the methodological details of the RNA analysis. Owing to the technical challenge of unambiguously distinguishing microglia from

dendritic cells (DCs) in brain cell suspensions, we employed a strategy of isolating 3-5 cells per pool and quantifying the relative expression of the microglia-specific marker *ccl34b.1* normalized to the DC-specific marker *ccl19a.1*. This approach aimed to reduce DC contamination in downstream analyses. Across all experimental groups subjected to RNA-seq analysis, the *ccl34b.1*/*ccl19a.1* expression ratios exceeded 5, confirming microglia as the dominant cell population. Nonetheless, residual DC contamination in the RNA-seq data cannot be entirely ruled out. We will explicitly acknowledge this technical constraint in the revised manuscript to ensure methodological transparency.

> *(2) The authors conclude that the reduction of microglia observed in the adult brain after cKO of pu.1 in the spi-b mutant background is due to apoptosis (Lines 213-215). However, they only provide evidence of apoptosis in 3-5 dpf embryos, a stage at which loss of pu.1 alone does lead to a complete loss of microglia (Figure 2E). A control of pu.1 KI/d839 mutants treated with 4OHT should be added to show that this effect is indeed dependent on the loss of spi-b. In addition, experiments should be performed to show apoptosis in the adult brain after cKO of pu.1 in spi-b mutants as there seems to be a difference in the requirement of pu.1 in embryonic and adult stages.*

We apologize for the omission of data regarding conditional *pu.1* knockout alone in the embryos in our manuscript which may have led to ambiguity. We would like to clarify that conditional *pu.1* knockout alone at the embryonic stage does not induce microglial death (Author response image 1). Microglial death occurs only when Pu.1 is disrupted in the *spi-b* mutant background, in both embryonic and adult brains. The blebbing morphology of some microglia after *pu.1* conditional knock out in adult *spi-b* mutant indicated microglia undergo apoptosis at both embryonic (Figure S4) and adult stages Author response image **2**). The reviewer's concern likely arises from the distinct outcomes of global *pu.1* knockout (Figure 2) versus conditional *pu.1* ablation. Global knockout eliminates microglia during early development due to Pu.1's essential role in myeloid lineage specification. We plan to include this clarification in the revised manuscript.

Author response image 1.

Conditional depletion of Pu.1 in embryonic microglia had no effect for their short-term survival. (A) Schematics of 4-OHT treatment for $pu.1^{KI/WT}$ *Tg(coro1a:CreER)* and $pu.1^{KI/\Delta 839}$ *Tg(coro1a:CreER)* at embryonic stage. (B) Representative images of $DsRed^{+}$ microglia in $pu.1^{KI/WT}$ and $pu.1^{KI/\Delta 839}$ at 5 dpf. (C) Quantification of $DsRed^{+}$ microglia in $pu.1^{KI/WT}$ and $pu.1^{KI/\Delta 839}$ at 3 dpf and 5 dpf. Values represent means ± SD, n.s., P >0.05.

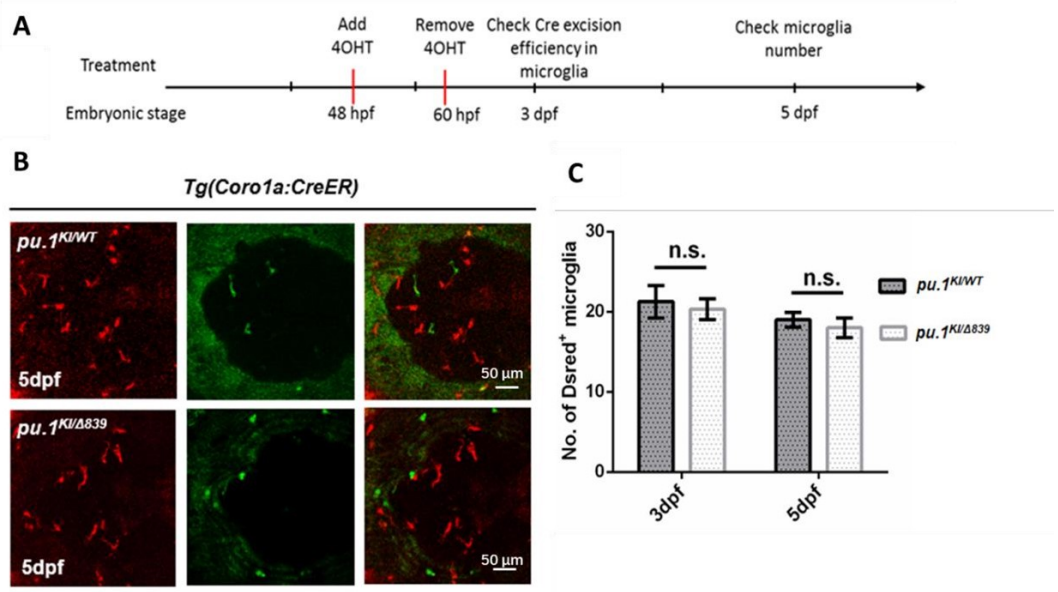

Author response image 2. Simultaneous inactivation of Pu.1 and Spi-b lead to microglia death in adult zebrafish. (A) The experimental setup for *pu.1* conditional knockout in adult *spi-b*$^{\Delta 232/\Delta 232}$ mutants (B) the representative images of the midbrain cross section of adult *pu.1*$^{KI/+}$*;spi-b*$^{\Delta 232/\Delta 232}$*;Tg(coro1a:CreER)* and *pu.1*$^{KI/WT}$*spi-b*$^{\Delta 232/\Delta 232}$*;Tg(coro1a:CreER)* fish at 2 dpi. The white arrow indicates microglia with blebbing morphology.

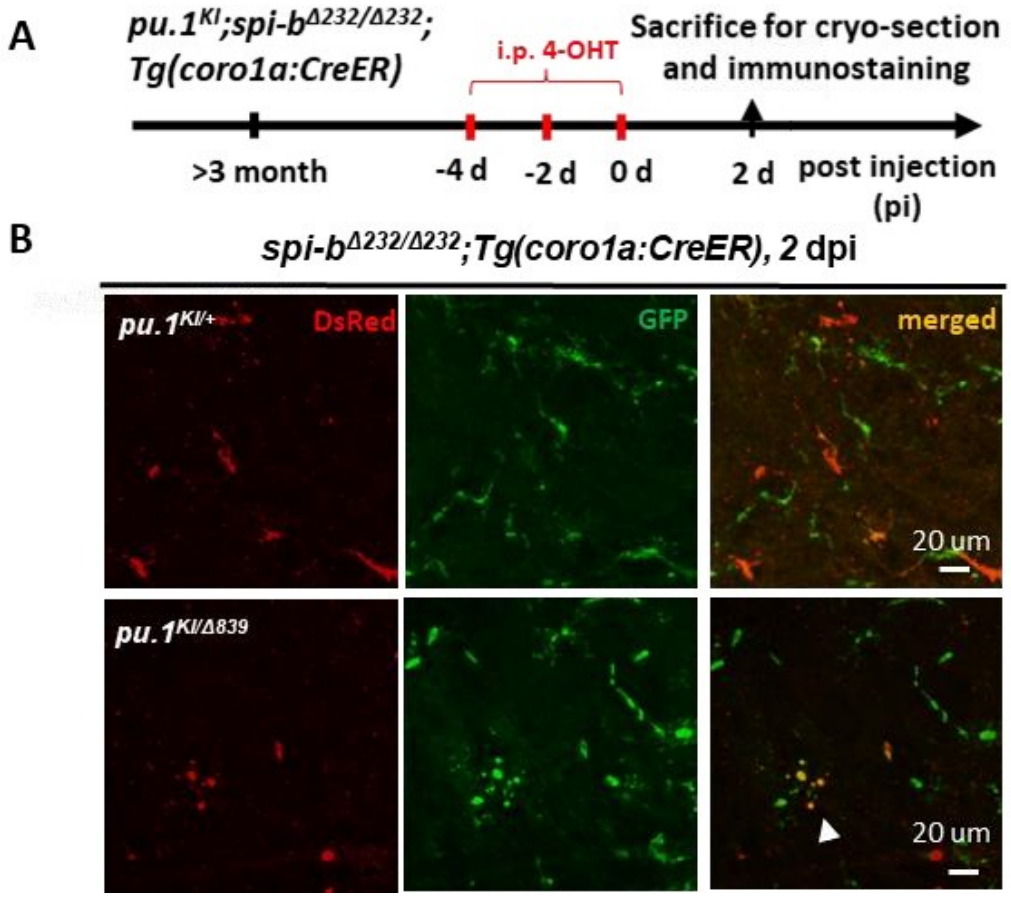

> *(3) The number of microglia after pu.1 knockout in zebrafish did only show a significant decrease 3 months after 4-OHT injection, whereas microglia were almost completely depleted already 7 days after injection in mice. This major difference is not discussed in the paper.*

We propose that zebrafish Pu.1 and Spi-b function cooperatively to regulate microglial maintenance, analogous to the role of PU.1 alone in mice. This cooperative mechanism likely explains the observed difference in microglial depletion kinetics between zebrafish and mice following *pu.1* conditional knockout. Specifically, the compensatory activity of Spi-b in zebrafish may buffer the immediate loss of Pu.1, whereas in mice, the absence of *SPI-B* expression in microglia eliminates this redundancy, resulting in rapid microglial depletion. Furthermore, during evolution, *SPI-B* appears to have acquired lineagespecific roles, becoming absent in microglia. We will expand on this evolutionary divergence and its implications for microglial regulation in the revised manuscript.

> *(4) Data is represented as mean +/-.SEM. Instead of SEM, standard deviation should be shown in all graphs to show the variability of the data. This is especially important for all graphs where individual data points are not shown. It should also be stated in the figure legend if SEM or SD is shown*

We plan to represent our data as mean ± SD in the revised manuscript.

Reference:

(1) Tschan MP, Reddy VA, Ress A, Arvidsson G, Fey MF, Torbett BE. PU.1 binding to the p53 family of tumor suppressors impairs their transcriptional activity. Oncogene. 2008 May 29;27(24):3489-93.

https://doi.org/10.7554/eLife.105788.1.sa0